INEEL/EXT-02-01330

Feasibility Study of Supercritical Light Water Cooled Fast Reactors for Actinide Burning and Electric Power Production

September 2002

Idaho National Engineering and Environmental Laboratory
Bechtel BWXT Idaho, LLC

INEEL/EXT-02-01330

Feasibility Study of Supercritical Light Water Cooled Fast Reactors for Actinide Burning and Electric Power Production

Nuclear Energy Research Initiative Project 2001-001

Progress Report for Work Through September 2002

4th Quarterly Report and 1st Annual Report

Principal Investigators: ***Philip MacDonald, Dr. Jacopo Buongiorno, Cliff Davis, and Dr. Kevan Weaver***
Telephone: 208-526-9634
Fax: 208-526-2930
Email: pem@inel.gov

Collaborating Organizations:

Massachusetts Institute of Technology
Principal Investigators: Professor Ron Latanision and Dr. Bryce Mitton

University of Michigan
Principal Investigator: Professor Gary Was

Westinghouse Electric Company
Principal Investigators: Drs. Luca Oriani, Mario Carelli, and Dmitry Paramonov, and Lawrence Conway

Table of Contents

Project Description

The use of light water at supercritical pressures as the coolant in a nuclear reactor offers the potential for considerable plant simplification and consequent capital and O&M cost reduction compared with current light water reactor (LWR) designs. Also, given the thermodynamic conditions of the coolant at the core outlet (i.e. temperature and pressure beyond the water critical point), very high thermal efficiencies of the power conversion cycle are possible (i.e. up to about 45%). Because no change of phase occurs in the core, the need for steam separators and dryers as well as for BWR-type re-circulation pumps is eliminated, which, for a given reactor power, results in a substantially shorter reactor vessel and smaller containment building than the current BWRs. Furthermore, in a direct cycle the steam generators are not needed.

If no additional moderator is added to the fuel rod lattice, it is possible to attain fast neutron energy spectrum conditions in a supercritical water-cooled reactor (SCWR). This type of core can make use of either fertile or fertile-free fuel and retain a hard spectrum to effectively burn plutonium and minor actinides from LWR spent fuel while efficiently generating electricity. One can also add moderation and design a thermal spectrum SCWR. The Generation IV Roadmap effort has identified the thermal spectrum SCWR (followed by the fast spectrum SCWR) as one of the advanced concepts that should be developed for future use. Therefore, the work in this NERI project is addressing both types of SCWRs.

This reactor concept presents several technical challenges. The most important are listed below.

1) Fuel and Reactor Core Designs:

- Local or total coolant voiding in the fast-spectrum SCWRs increases leakage, but hardens the neutron energy spectrum and decreases parasitic absorption. The net effect can be a reactivity increase. The core must be designed to ensure that the overall reactivity coefficient is negative.
- The thermal-spectrum SCWRs require additional moderation, water rods can be used but one has difficult design problems to control the heat transfer from the coolant to the moderator rods, especially during off-normal and accident situations. A solid moderator might be better.
- A low conversion ratio fuel rapidly loses reactivity with burnup, thus requiring a large excess reactivity at beginning-of-life to operate continuously for an acceptably long time. Therefore, a control system must be designed that safely compensates for reactivity changes throughout the irradiation cycle, or the spectrum must be hardened to increase the conversion ratio.
- The Doppler feedback in the fast-spectrum SCWRs will be much smaller than that found in typical LWRs.

2) Fuel Cladding and Structural Material Corrosion and Stress Corrosion Cracking:

- Because of the oxidizing nature of high temperature water, corrosion and stress corrosion cracking of the fuel cladding and core internals materials are expected to be major concerns for this reactor concept.
- Radiolysis of the water coolant in the fast-spectrum SCWRs may take place at a higher rate than in traditional LWRs. In addition, the radicals formed by the radiolytic decomposition of the water (both fast and thermal versions) are highly soluble in supercritical water and may not recombine as well as in an LWR.
- The hard neutron spectrum in the fast-spectrum SCWRs makes the irradiation damage of the fuel cladding and core structural materials more pronounced than in traditional LWRs. Also, high-

energy neutrons work as catalysts for the oxidation and stress corrosion cracking of the structural materials (irradiation assisted stress corrosion cracking).

3) Plant Engineering and Reactor Safety Analysis:

- A direct cycle solution has been selected as reference for this study. However, the proposed direct cycle features a once-through vessel and core design, different from the typical BWR recirculation system. The effect of this choice on the operational stability and on the safety response of the system needs to be evaluated.
- For the alternative solution of an indirect cycle, loop PWR components (steam generators, reactor coolant pumps, and eventually pressurizer) need to be developed.
- Because of the significant coolant density variation along the core, the supercritical water reactor might be susceptible to coupled neutronic/thermal-hydraulic instabilities.
- Because of the large enthalpy rise along the core, the supercritical water reactor requires that radial peaking factors and hot channel factors be minimized. Also, the system will be more sensitive to operational and accident variations in operating parameters, and the implication on safety of this characteristic needs to be thoroughly assessed.
- Due to the adoption of canned assemblies, the system might be susceptible to parallel channel instabilities.
- The response of the plant to design and anticipated transients might differ significantly from that of LWRs and needs to be evaluated.

The project is organized into three tasks, reflecting the three technical challenges above.

Task 1. Fuel-cycle Neutronic Analysis and Reactor Core Design (INEEL). For the fast-spectrum SCWR, metallic and oxide fertile fuels will be investigated to evaluate the void and Doppler reactivity coefficients, actinide burn rate, and reactivity swing throughout the irradiation cycle. Although metallic alloy fuels are incompatible with the water coolant, we envision the use of a dispersion type of metallic fuel, which will be compatible with water. Included in the fertile options will be the use of thorium. The main variables are the core geometry (e.g. fuel rod length, pitch-to-diameter ratio, assembly configuration) and the fuel composition. For the thermal-spectrum SCWR, a variety of fuel and moderator types will be assessed. The MCNP code will be utilized for instantaneous reactivity calculations and the MOCUP code for burnup calculations and isotopic content.

Task 2. Fuel Cladding and Structural Material Corrosion and Stress Corrosion Cracking (University of Michigan and MIT). The existing data base on the corrosion and stress-corrosion cracking of austenitic stainless steel and nickel-based alloys in supercritical water is very sparse. Therefore, the focus of this work will be corrosion and stress corrosion cracking testing of candidate fuel cladding and structural materials. In Year 1 of the project MIT will use an existing supercritical-water loop to conduct initial corrosion experiments on a first set of candidate alloys in flowing supercritical water, and will identify promising candidate alloys classes for core internal components and fuel cladding based on existing data on the alloys radiation stability and resistance to both corrosion and stress-corrosion cracking. A high temperature autoclave containing a constant rate mechanical test device will be built and tested in Year 1 and operated in Years 2 and 3 at the University of Michigan. The resulting data will be used to identify promising materials and develop appropriate corrosion and stress corrosion cracking correlations.

Task 3. Plant Engineering and Reactor Safety Analysis (Westinghouse and INEEL). The optimal configuration of the power conversion cycle will be identified as a function of the plant mission (e.g. pure electricity generator, co-generation plant, hydrogen generator). Particular emphasis will be given to the

applicability of current supercritical fossil-fired plant technology and experience to a direct-cycle nuclear system. A steady-state sub-channel analysis of the reactor core will be undertaken with the goal of establishing power limits and safety margins under normal operating conditions. Also, the reactor susceptibility to coupled neutronic/thermal-hydraulic oscillations will be evaluated. The response of the plant to accident situations and anticipated transients without scram will be assessed. In particular the following transients and accidents will be analyzed: start-up, shut-down, load change and load rejection; LOCAs and LOFAs. As part of this analysis, a suitable containment design will be explored to mitigate the consequences of LOCA accidents.

Task 1 Results: Assessment of Solid Moderators for Thermal Spectrum SCWRs (Dr. Jacopo Buongiorno, INEEL)

1.1. Summary of Previous Work

During the 1st quarter, a qualitative analysis was performed to determine which fuel form would support the highest reactivity-limited burnup in a fast-spectrum SCWR, and would have the most proliferation resistant isotopics at a particular burnup. A relatively long core life and a modest reactivity swing are possible in fast-spectrum SCWRs with most fuels. However, the uranium-based fuel types had the highest beginning-of-life reactivity, and the best reactivity-limited burnup, whereas the thorium-based fuels had the best spent-fuel isotopics. Therefore, the most appropriate fuel for fast-spectrum SCWRs appears to be a mixture of thorium and uranium to balance long core life with proliferation resistant isotopics.

Work was started during Quarter 2 to assess the design of a thermal-spectrum SCWR, in part, because of the emphasis the Generation IV Roadmap has put on the need to first develop a thermal-spectrum SCWR, before developing a fast-spectrum version. In order to thermalize the neutron spectrum in a supercritical pressure water reactor, one can increase the pin pitch or introduce moderator rods to increase the moderator to fuel ratio. While increasing the pin pitch would be the simplest approach, the large hydraulic diameter would result in very low coolant velocities and unacceptable cladding temperatures. Therefore, one must employ moderator rods or cans and initial calculations were performed to verify the moderating power of several different moderators including water, zirconium hydride, graphite, and beryllium.

The analyses of the neutronic performance of several solid moderators for the SCWR core was continued in the 3rd quarter and the results compared to that of water rods. It was found that the only acceptable solid moderator is δ-phase zirconium hydride ($ZrH_{1.6}$), which generates a relatively high multiplication factor and a negative coolant void reactivity coefficient. The beginning-of-life reactivity results are illustrated in Figure 1 in terms of the multiplication factor, k_{eff}. The multiplication factor for a PWR fuel pin with Zircaloy-4 cladding and for a fictitious PWR pin with Alloy 718 cladding are also shown in Figure 1. From Figure 1 it is apparent that among the SCWR moderators water performs best reactivity-wise, closely followed by $ZrH_{1.6}$. The other solid moderators exhibit significantly lower reactivity, with BeO and SiC performing worse than Be and C, respectively. Also, a comparison of the two PWR cases suggests that the reactivity penalty associated with the use of Alloy 718 instead of the low-absorbing Zircaloy-4 is significant. However, this penalty is an intrinsic characteristic of the SCWR (for which zirconium alloys cannot be used because of their low strength at high-temperature) and thus is not instrumental in discriminating between moderators.

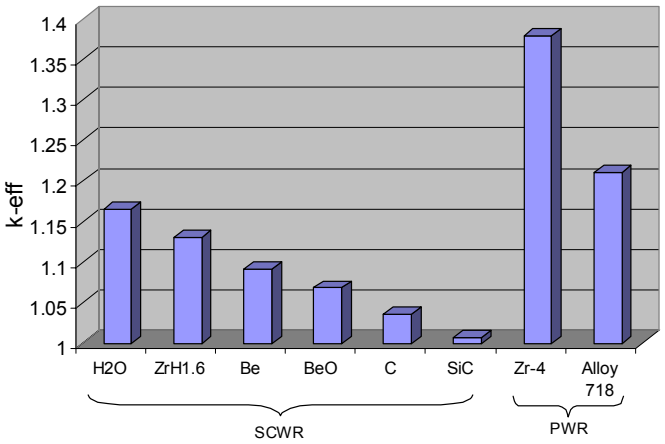

Figure 1. Beginning-of-life reactivity performance of cores with various moderator material.

Several issues key to the chemical and thermo-mechanical feasibility of $ZrH_{1.6}$ were assessed during the 3rd quarter including zirconium-hydride/water interaction, hydrogen release, hydrogen redistribution, pressurization of the moderator box at high temperature, phase stability, and compatibility of zirconium hydride with the moderator box material. It was found that:

1) The chemical reaction of zirconium hydride with water is thermodynamically favored but kinetically impaired even at high temperatures.
2) Hydrogen release is low at steady-state, while the use of a hydrogen-impermeable coating on the inner surface of the moderator box might be required at higher temperatures.
3) The moderator-box wall temperature during a LOCA should be limited to 900°C to prevent failure from internal hydrogen pressure.
4) Hydrogen redistribution and release do not threaten the stability of δ-phase zirconium hydride.
5) The use of a solid moderator greatly enhances the thermal capacity of the SCWR core.
6) The issues of hydriding and hydrogen embrittlement of the moderator box material, Alloy 718, appear of little concern, while high-temperature diffusion of zirconium into Alloy 718 might have to be prevented by means of a thin molybdenum protective coating.
7) Finally, fabrication of the SCWR moderator rods appears feasible within the envelope of existing technology.

In the cost area a simple analysis indicated that the use of zirconium-hydride moderator will not result in significant economic penalization of the SCWR.

This work was continued in the 4th Quarter as discussed below.

1.2. Axial Peaking Calculations

The density of SCW varies greatly with temperature. As such, the axial coolant-density profile depends on the temperature profile and thus on the power profile. In turn, the power profile depends on the density profile because of the coolant effect on neutron moderation. Therefore, in general the neutronics and thermal-hydraulics of the SCWR core are coupled, although this coupling effect is somewhat reduced for a core in which most of the moderation is provided by a solid moderator.

The geometry of the SCWR core cell with zirconium-hydride moderator is illustrated in Figure 2 (note that the dimensions in Figure 2 have been adjusted slightly and the current values are presented in Section 3, but the values shown here were the ones used in the neutronic analyses). The conceptual feasibility of this concept was reported in the previous quarterly report. The active fuel length is 4.27 m. A fission gas plenum of about 40 cm is provided at the top of the fuel pins. The fuel is UO_2 at 95% theoretical density (~10.42 g/cm^3). The fuel cladding and moderator box wall are made of Alloy 718 with a density of 8.19 g/cm^3. The moderator is $ZrH_{1.6}$ with a density of 5.64 g/cm^3. The lower and upper reflectors of 3 cm thickness each are also made of Alloy 718. The lower and upper coolant plena were modeled as semi-infinite volumes filled with

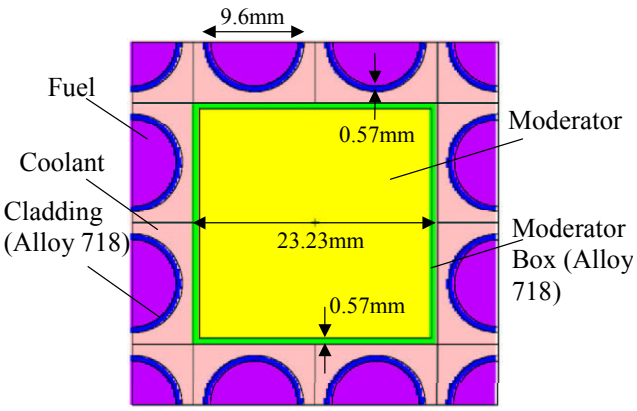

Figure 2. Cross-sectional view of the core cell with moderator box.

coolant of density corresponding to the core inlet and outlet temperature, respectively. Therefore, the axial leakage was accounted for. On the other hand, the cell vertical boundaries were modeled as perfectly reflective. The neutronic calculations were performed with the Monte Carlo code MCNP4B. The number of neutron histories followed for each run was 4×10^6. In order to input the coolant density profile and calculate the axial power profile, the coolant and fuel pin regions were divided into 40 axial zones each.

The enthalpy profile in the coolant channel was calculated by means of a simple energy balance:

$$\dot{m}\frac{dh}{dz} = q'(z) \qquad (1)$$

where $\dot{m}$ is the channel flow rate, h is the coolant enthalpy, q' is the linear heat generation rate (i.e., the axial power profile). To solve Equation (1), it was assumed that the inlet and outlet temperatures are 280 and 450°C, respectively, the reactor pressure is 25 MPa and the total power per fuel pin is 100 kW. Then the density and temperature profiles were calculated from the known enthalpy-temperature and enthalpy-density relations for SCW.

The thermal-hydraulic and neutronic models were used iteratively until the power profile converged within 1% from one iteration to the next. The reference case with uniform 4% U-235 enrichment was analyzed first and is illustrated in Figure 3. It can be seen that the axial peaking in the lower half of the core is unacceptably high, i.e., the peaking factor is about 2.3. Then, a two- zone approach with 4.2% enrichment in the upper half of the core and 4% enrichment in the lower half was evaluated. The results are also shown in Figure 3. The reduction in the axial peaking is rather dramatic, as the new peaking factor is about 1.4, i.e., actually smaller than for a classic chopped-cosine profile. This will result in a higher achievable average discharge burnup, which reduces fuel costs, and will also drastically reduce the peak temperature on the cladding, as shown in Figure 4. The peak cladding temperature decreases from 784°C (uniform enrichment case) to 494°C (two-zone case). This will provide for larger design and safety margins. It is emphasized that these remarkable results are obtained with a simple two-zone approach with minimal enrichment differential between the two zones. However, optimization should be possible to flatten the axial power profile even further (e.g., with a three-zone approach). The curves of Figure 4 were generated by means of Equation (1) and the Oka-Koshizuka heat-transfer-coefficient correlation, which accounts for the deterioration of heat transfer phenomena typical of SCWRs. The Oka-Koshizuka correlation is also described in the previous quarterly report.

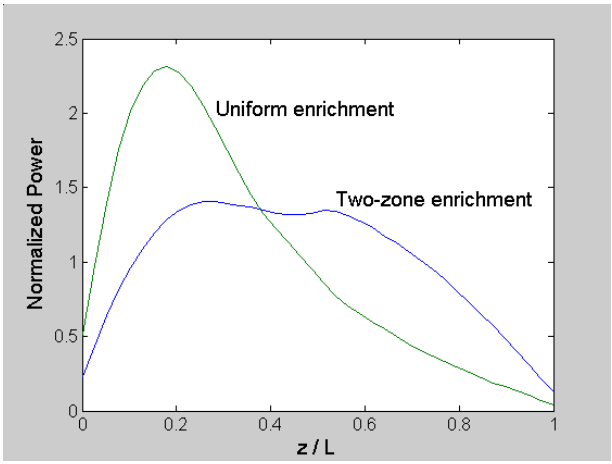

Figure 3. Axial power profile in the SCWR.

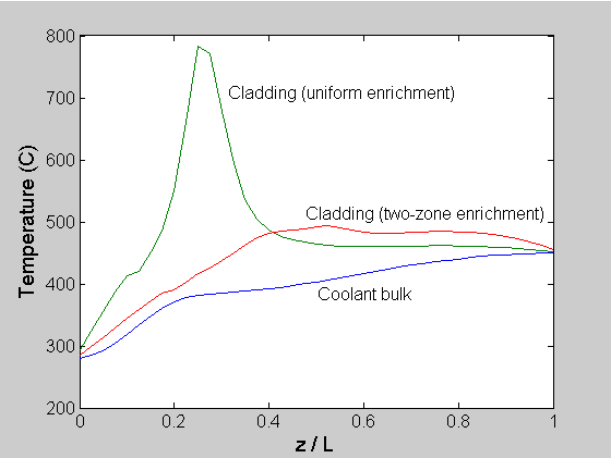

Figure 4. Axial temperature profiles in the SCWR.

1.3. Doppler Feedback

The Doppler feedback for the SCWR with solid moderator was evaluated with the temperature dependent cross-section libraries of MCNP4B. These are the ENDF-B/VI libraries for room temperature modified with the NJOY cross-section processing code for higher temperatures. The number of neutron histories followed was 4×10^5. First the multiplication factor k_{eff} was calculated for the core cell of Figure 2 with the fuel (U-238 and U-235) at room temperature, 293 K; second, the calculation was repeated for the fuel at 880 K. The results were as follows: at 293 K k_{eff}=1.135±0.001, at 880 K k_{eff}=1.119±0.001. Thus, the average Doppler coefficient, α_T, over the 293-880 K range can be calculated as

$$\alpha_T \approx \frac{\rho(T_2)-\rho(T_1)}{T_2-T_1} \approx -2.1 \text{ pcm/K} \qquad (2)$$

where $\rho=(k_{eff}-1)/k_{eff}$ is the neutron reactivity, T_2=880 K and T_1=293 K. This value falls within the typical range for LWRs (i.e., from -4 to -1 pcm/K), as reported by Duderstadt and Hamilton [1976], and thus is deemed acceptable.

1.4. Local Peaking and Sub-channel Considerations

The power distribution within a fuel assembly was also calculated. A schematic of the SCWR fuel assembly with zirconium-hydride moderator boxes is shown in Figure 5. It is of the 19×19 type closed by an external duct wall for isolation from the contiguous assemblies. Assembly ducting, also adopted in BWRs and LMRs, is necessary for the SCWR core because the coolant flow rate for each assembly has to be controlled to match the power in order to prevent excessive temperature rises in the core, as explained in the previous quarterly report. The geometry of the fuel pins and moderator boxes is that of Figure 2, the duct wall is made of Alloy 718 and its thickness is 0.57 mm, while the gap between contiguous assemblies is 10 mm wide. The gap, which fills up with slow-flowing water during operation, was sized to accommodate cruciform control rods of the BWR type and to provide adequate moderation for the peripheral fuel pins, which face only one zirconium-hydride box. Rationale for the cruciform control rods is presented in Section 1.5 below.

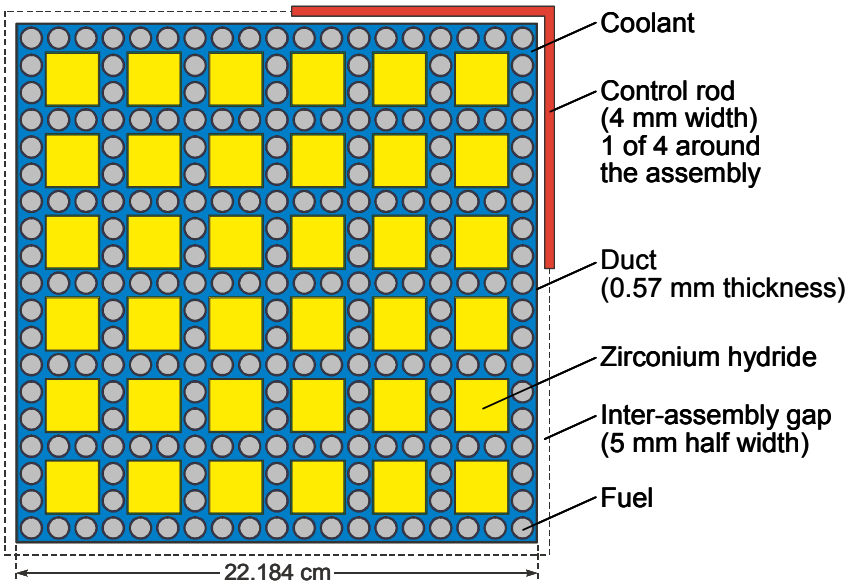

Figure 5. The SCWR 19×19 fuel assembly with solid moderator.

The power distribution within the assembly was also calculated by means of the MCNP4B code with 1.2×10^7 neutron histories. This high number of histories was needed to reduce the uncertainty on the

usually-small local power peaking. Because of its symmetry, only 1/8 of the assembly was modeled, as illustrated in Figure 6, in which the reflective surfaces are described by dashed lines. For the local peaking calculations the control rods were completely withdrawn from the inter-assembly gap, and the gap was filled with SCW with a density of 0.78 g/cm^3. The two-axial-zone enrichment approach was maintained, while all other assumptions are identical to the cell calculations of Section 1.2. The results are also shown in Figure 6 where the normalized power for each fuel pin is reported. The MCNP-calculated uncertainty for this output is ±0.1%, i.e., on the third decimal of the normalized power. For the sake of convenience, we shall number the fuel pins according to their position in the lattice. Therefore, the pin at the center of the assembly (Row 1, Column 1) will be labeled (1,1), that at the upper right corner of the assembly will be labeled (10,10), and so forth. It can be seen that the power distribution is relatively flat with a local peaking factor of 1.108. The pins at the four corners of the moderator boxes (e.g., pins (1,1), (4,1), (4,4), (7,4), etc.) generally exhibit lower power, which is expected because these pins are subject to worse moderation than the pins "sandwiched" between two moderator boxes (e.g., pins (2,1), (3,1), (4,2), (7,5), etc.). Also, the peripheral pins (i.e., (10,1) through (10,10)) appear to be well moderated, which corroborates the choice of a relatively wide inter-assembly gap. Pins (10,8), (10,9) and (10,10) actually have a somewhat higher power due to their proximity to the intersection of 4 inter-assembly gaps full of water.

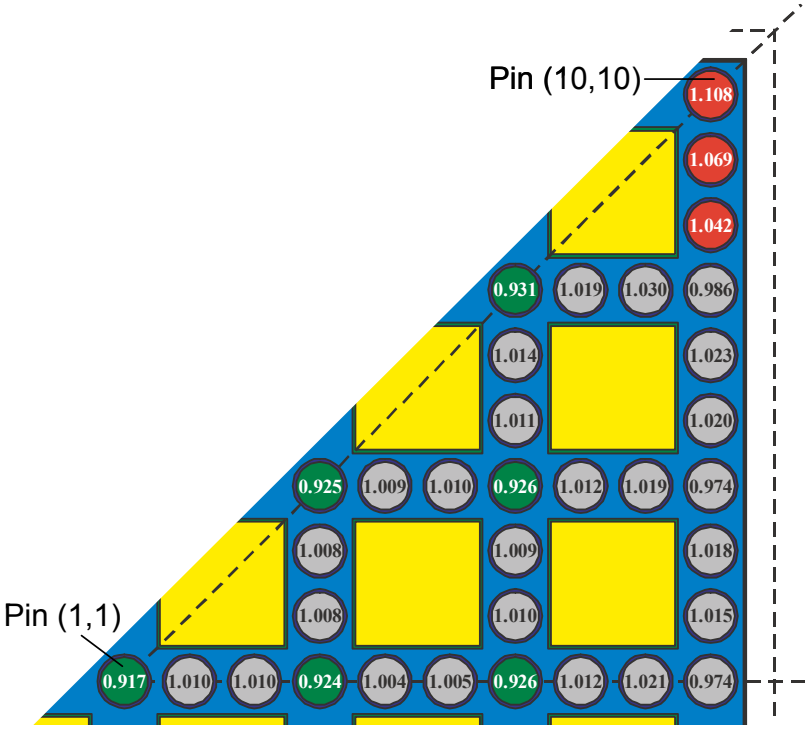

Figure 6. Power distribution within the SCWR fuel assembly with solid moderator.

Even though the calculated local peaking is not very high, it is desirable to further reduce it. This is particularly important in a SCWR fuel assembly where small power differences between channels can result in large differences in the outlet temperatures. A convenient way to flatten the power distribution within the assembly is to adjust the enrichment from pin to pin. This approach is currently used in BWRs where in each fuel assembly there can be up to 4 different enrichment levels [Knief 1992]. To assess the number of enrichment levels required for the SCWR, let us first consider the square cell around each fuel pin. The coolant enthalpy (temperature) rise in the generic cell (i,j) can be calculated as:

$$\Delta h_{ij} = \frac{\dot{q}_{ij}}{\dot{m}_{ij}} \tag{3}$$

where $\dot{q}_{ij}$ and $\dot{m}_{ij}$ are the power generated and the coolant mass flow rate associated with fuel pin (i,j), respectively. The pressure drop in each cell can be calculated as:

$$\Delta P_{ij} = K \frac{\dot{m}_{ij}^2}{2\rho_{ij} A_{ij}^2} \tag{4}$$

where ρ_{ij} is the average coolant density, A_{ij} is the cell flow area and K is the pressure drop coefficient, assumed constant for simplicity. Because all cells are hydraulically connected to the same upper and lower plena, the pressure drop in all cells must be the same, i.e., ΔP_{ij}=constant. Also, if we impose the temperature rise in all cells to be the same (i.e., Δh_{ij}=constant), Equations (3) and (4) can be combined to yield:

$$\frac{\dot{q}_{ij}}{A_{ij}} = \text{constant} \tag{5}$$

Equation (5) represents the condition for uniform temperature distribution throughout the assembly. However, note that the flow area for all cells is the same (they are all square cells with a fuel pin in the center), so equation (5) ultimately becomes:

$$\dot{q}_{ij} = \text{constant} \tag{6}$$

Thus, the condition for uniform temperature distribution in the fuel assembly is that all fuel pins generate roughly the same power. Assuming that, for a given pin, the power output is proportional to the enrichment, a direct inspection of Figure 6 indicates that:

1) The enrichment must be increased by about 7 to 8% in pins (1,1), (4,1), (7,1), (4,4), (7,4) and (7,7),
2) Nominal enrichment can be maintained in pins (2,1), (3,1), (5,1), (6,1), (8,1), (9,1), (10,1), (4,2), (4,3), (5,4), (6,4), (7,2), (7,3), (7,5), (7,6), (8,4), (8,7), (9,4), (9,7), (10,2), (10,3), (10,4), (10,5), (10,6) and (10,7),
3) The enrichment must be reduced by 5 to 10% in pins (10,8), (10,9) and (10,10).

Therefore, the SCWR fuel assembly would have three groups of pins with different enrichment levels. The enrichment levels are marked in different colors in Figure 6.

This analysis is based on very simplified assumptions and gives only preliminary indications regarding the flow and temperature distributions within the assembly. In reality, the pressure drop coefficient is not constant but depends on the hydraulic diameter and coolant velocity in each cell. Also, cross flow between contiguous cells, which was neglected here, changes the flow and temperature distributions, and the reactivity feedback plays an important role as well. A complete sub-channel analysis will be required to actually design the SCWR fuel assembly and evaluate its performance. This issue will be addressed in the near future with the modified version of the VIPRE code being developed at Westinghouse.

1.5. Control Rods and Reactivity Inventory

The reference control rods for the SCWR core with solid moderator are cruciform type control rods similar to the control rods of a BWR. However, contrary to the BWR, the rods are inserted from the top of the core. The selection of inter-assembly control rods over PWR-type in-assembly control rodlets was driven mainly by three considerations, as explained next. First, a gap between assemblies is needed to provide moderation for the peripheral fuel pins, so room is already available to insert the control rods; second, having the rods in the inter-assembly gap does not disturb the coolant flow within the assembly; and third, the rods displace a significant amount of high-density water upon insertion, which increases their worth. There is one rod per fuel assembly, or roughly one rod per 500 cm^2, which is comparable with the control rod "density" in a BWR. Note that in a BWR there is only one rod every 4 assemblies, but area-wise the assemblies are about 4 times smaller than for the SCWR, and thus the number of control rods per unit core area (or, for a given core diameter, the total number of control rods) comes out about the same. The neutron absorbing material is natural boron carbide. The total worth of the control rods was calculated by comparing the multiplication factor for two cases: all rods withdrawn and all rods fully inserted. The results are as follows: all rods withdrawn k_{eff}=1.141±0.001, all rods fully inserted k_{eff}=0.807±0.001. Thus the total control rod worth, $\Delta\rho_{CR}$, is:

$$\Delta\rho_{CR} = \rho_{in}-\rho_{out} \sim -36{,}200 \text{ pcm} \quad (7)$$

where again ρ is the neutron reactivity and the subscripts "in" and "out" refer to the all-rods-inserted and all-rods-withdrawn cases, respectively.

It was then possible to calculate the reactivity margin at cold shutdown. Assuming a temperature drop of about 800 K in the fuel between normal operating conditions and cold shutdown, the reactivity gain from Doppler effect is about 1,700 pcm (calculated from the value of α_T in Section 1.3). The reactivity gain from flooding the core with high-density coolant was reported in the previous quarterly and is about 800 pcm. Thus the total positive reactivity insertion is 2,500 pcm. It can be seen that the control rod worth is an order of magnitude larger than this value, thus providing adequate margin at cold shutdown, i.e., -33,700 pcm or -$48, assuming a delayed-neutron fraction of 700 pcm. In fact, given the large margin, it might be possible to significantly reduce the number of control rods, which might have a sizable impact on capital cost.

Task 2 Results: Fuel Cladding and Structural Material Corrosion and Stress Corrosion Cracking Studies

2.1. Progress of Work at MIT (Prof. Ron Latanision and Dr. Bryce Mitton)

2.1.1. Identification of the Most Promising Materials

As discussed in our third quarterly, Hattori et al. [2000] tested several candidate alloys (austenitic steels, nickel base alloys, Ti alloys, high Cr ferritic steels) in SCW at 566˚C, 25MPa, and in superheated steam at 566˚C, 12MPa. Their data suggests the potential for employing austenitic stainless steels (310, 316) or high nickel alloys (690, 718) as cladding materials. While the study at MIT will, ultimately, assess coupons of Alloy 316, 625, 690, 693, 718, HT9 and T91 (to be supplied by the University of Michigan), it was determined that preliminary experiments would be carried out on Alloy 316 and 625.

Alloy 316: A survey performed by CLI International regarding the selection of materials for the fabrication of a facility to treat waste by supercritical water oxidation reports general corrosion and excellent overall performance for AISI 316 stainless steel exposed to deionized water over a temperature range between 300 and 500˚C [Tebbal and Kane 1998]. Conversely, for similar conditions, localized corrosion has also been documented [Boukis et al. 1995, Mitton et al. 1995]. Pitting was observed for exposure periods on the order of 150 hours at a temperature of approximately 400˚C and a pressure of about 24.5 MPa [Mitton et al. 1995]. At temperatures between 300˚C and 500˚C for periods as long as 240 hours at a pressure of 24.8 MPa, intergranular corrosion (300˚C) and crevice corrosion at the periphery of a mounting washer (500˚C) have both been documented [Boukis et al. 1995]. Stress corrosion cracking was observed after exposure to deaerated supercritical water at 732˚C for approximately 168 hours at high pressures (103 MPa) [Boyd and Pearl 1965]. In the latter case, cracks were primarily transgranular and generally initiated at pits. Similar cracking phenomena were also observed after extended times (approximately 3600 hours) at a lower temperature (538˚C) [Boyd and Pearl 1965].

Alloy 625: At temperatures of 450-500˚C and exposure times between 150 and 240 hours, the general trend was for Alloy 625 to exhibit good performance [Tebbal and Kane 1998, Boukis et al. 1995] with the formation of a potentially protective film [Mitton et al. 1995]; however, pit development [Tebbal and Kane 1998, Mitton et al. 1995] was also observed. Grain boundary carbide precipitation has also been reported for Alloy 625 exposed to superheated steam at temperatures of 566 and 621˚C [Wozaldo and Pearl 1965]. At the lower temperature, carbides did not develop before approximately 2000 hours and were still small and discrete after 5800 hours. Precipitation was, however, heavy at the higher temperature, and large globular carbides were seen after 1000 hours. Stress corrosion cracking has also been observed in a Alloy-625 bellows exposed to oxygenated water at 288˚C [Berry 1973].

2.1.2. Corrosion and Stress Corrosion Cracking of Candidate Materials

Figure 7 presents a schematic representation of the current SCW facilities at MIT. (This facility was described in more detail in the first two quarterlies of this project.) The exposure facility on the right incorporates a relatively large autoclave with an internal volume of approximately 860 mls. It is large enough to expose a rack of weight loss, welded, and u-bend samples for extended times. There is also an "instrumented tube" exposure facility shown on the left.

The SEM micrographs in Figure 8 present the exposed surface of (a-b) an Alloy 625 and (c-d) an Alloy 316 sample after 171 hours exposure to (non-deaerated) deionized water at a temperature of 400˚C and pressure of 24 MPa. Non-deaerated deionized water refers to the oxygen concentration that would be reached for water freely exposed to the atmosphere. This condition would echo that referred to in Hattori's paper [2000] as the aerated condition. Subsequent to exposure, the surface of both (a) Alloy 625 and (c) Alloy 316 was generally covered by a tenacious oxide. For both alloys, however, some pit development was also observed. While the pit diameter is only on the order of 2.5 - 8 µm for Alloy 625 (Figure 8b) and approximately 2µm for the 316 stainless steel (Figure 8d), SCC can develop more readily at regions of stress concentration; thus, features such as pits must be regarded as potential sites for preferential crack initiation.

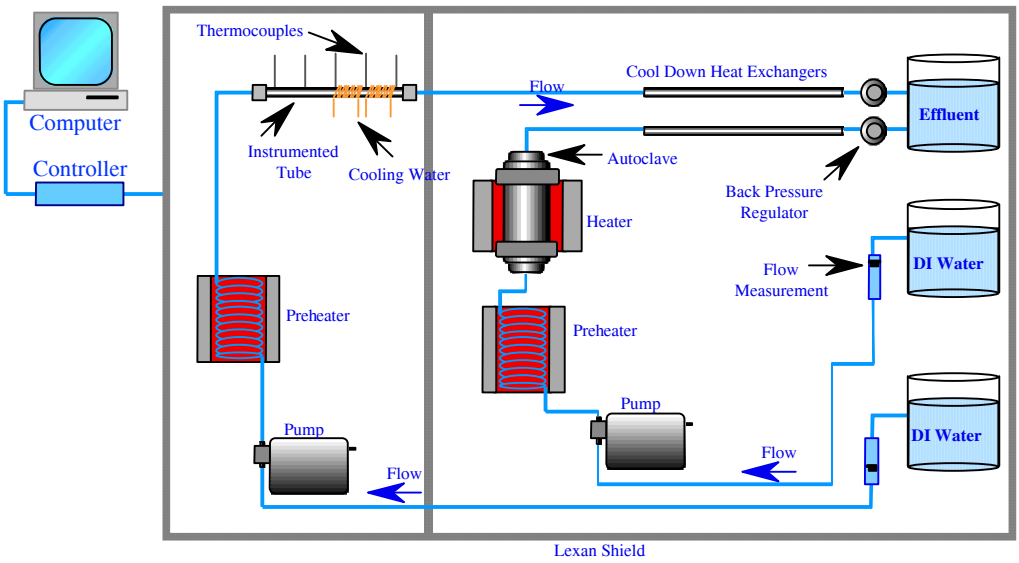

Figure 7. Schematic of the MIT SCW loop.

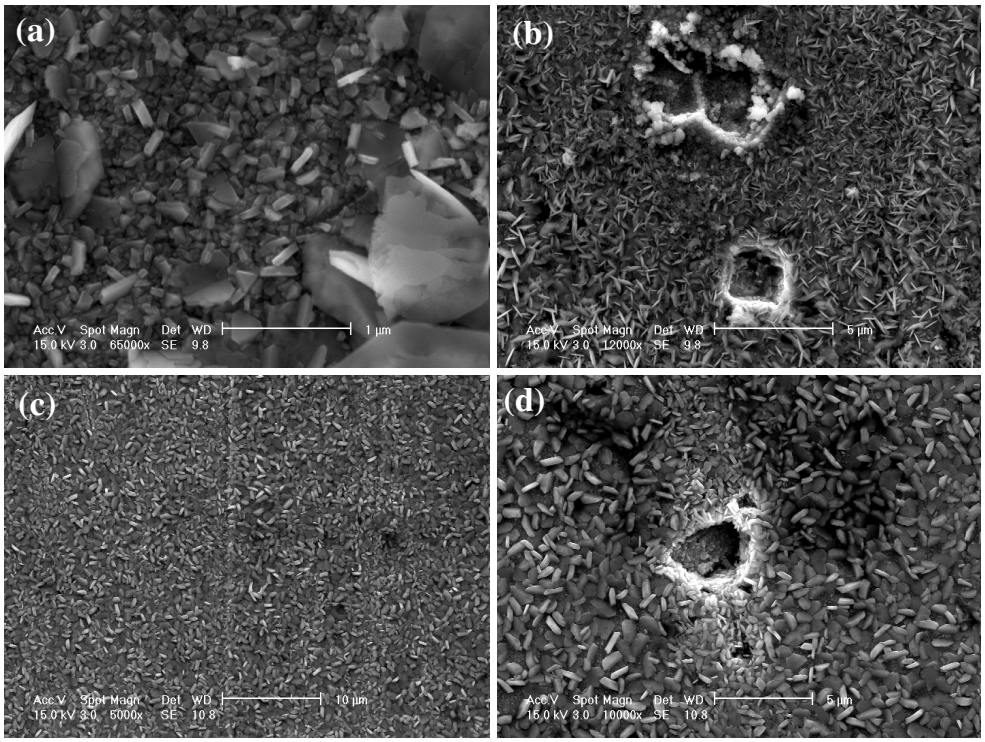

Figure 8. SEM micrographs of the exposed surfaces of (a-b) an Alloy 625 and (c-d) an Alloy 316 sample after 171 hours at 400˚C in non-deaerated deionized water.

Figure 9 reveals the surface of an Alloy 625 sample exposed to non-deaerated deionized water at 300˚C for 240 hours. The surface is primarily covered with an oxide; however, localized corrosion in the form of pit development is also apparent. In this case, the pit diameter is on the order of 10μm.

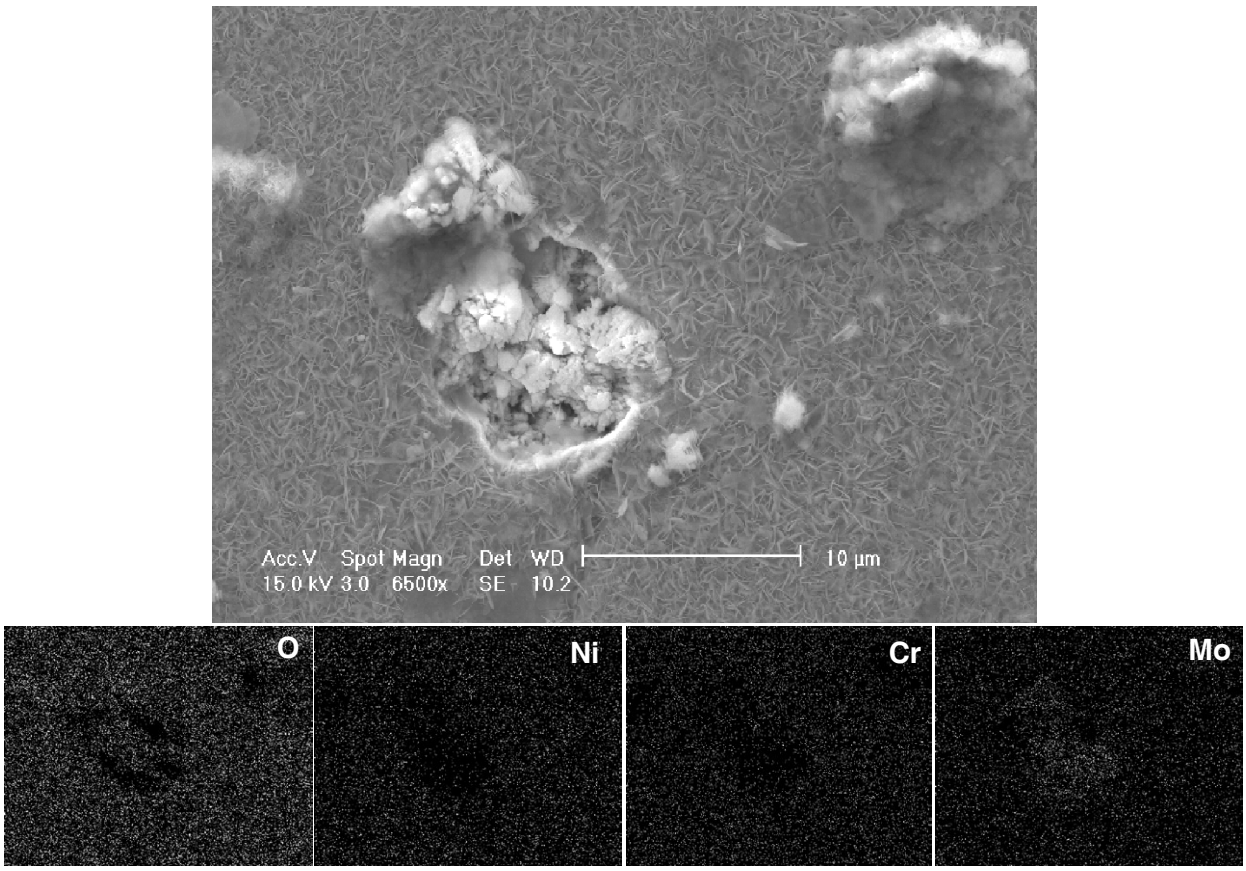

Figure 9. Elemental analysis and exposed surface of an alloy 625 sample after 288 hours at 300˚C in 15 mega ohm water.

The results of the elemental analysis shown in Figure 9 above suggest that the corrosion product within the pit exhibits an elevated Mo content. Interestingly, for similar exposure conditions, Hattori et al [2000] report a Mo rich layer for Alloy 316. Current samples will subsequently be mounted and viewed in cross section to better delineate the presence and location of any Mo rich layer.

System Modification: Preliminary tests for Alloy 625 and 316 will include experiments incorporating the instrumented tube design discussed in previous reports. A tube of the alloy to be tested is used as the autoclave and micro-thermocouples are attached externally along the length of the vessel. Water at an elevated temperature and pressure is pumped into one end and permitted to cool as it transverses the tube. For the current project, some redesign of the system has been required in order to achieve the significant temperature drop needed to obtain information on both the super- and sub-critical regimes at the same time. Figure 10 presents the current design, which includes water-cooling by external copper tubes coiled between the final two thermocouples. The temperatures recorded in this figure reflect the actual stable temperature measurement achieved during a preliminary test. Thus, it was possible to attain a temperature decrease in excess of 130˚C along the length of the tube. An experiment incorporating this design will be carried out shortly using a 316 stainless steel tube.

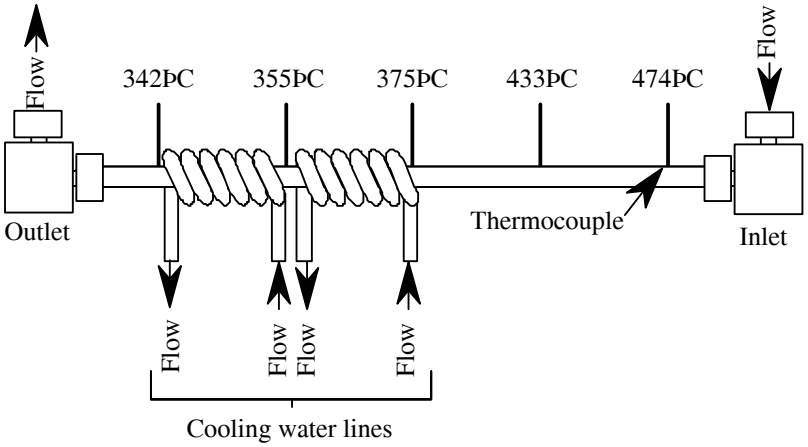

Figure 10. Instrumented-tube system modification.

2.2. Progress of Work at the University of Michigan (Prof. Gary Was)

The design and fabrication of the University of Michigan supercritical water loop system for stress corrosion cracking tests was completed during the first two quarters of this NERI project. In this loop system, one tensile sample can be tested in various loading modes such as constant extension rate tension (CERT), constant load, ramp and hold, low cycle fatigue, etc. Additionally, 6 U-bend samples can be loaded into the test vessel, using sample holders secured to the vessel internal support plate. Figure 11 shows a schematic of the water loop. Water is stored in a column with the amount of water controlled by addition of gas to the column. An ion exchanger is used to control the conductivity. The oxygen content is read at the exit of the column. The conductivity is read at room temperature both in the inlet and the outlet line. The water flows to an autoclave in which constant extension rate tensile (CERT) tests and U-bend tests can be performed at temperatures up to 550°C and under a pressure of up to 34.5 MPa. The temperature is read in the vessel and the pressure is read at room temperature in the inlet

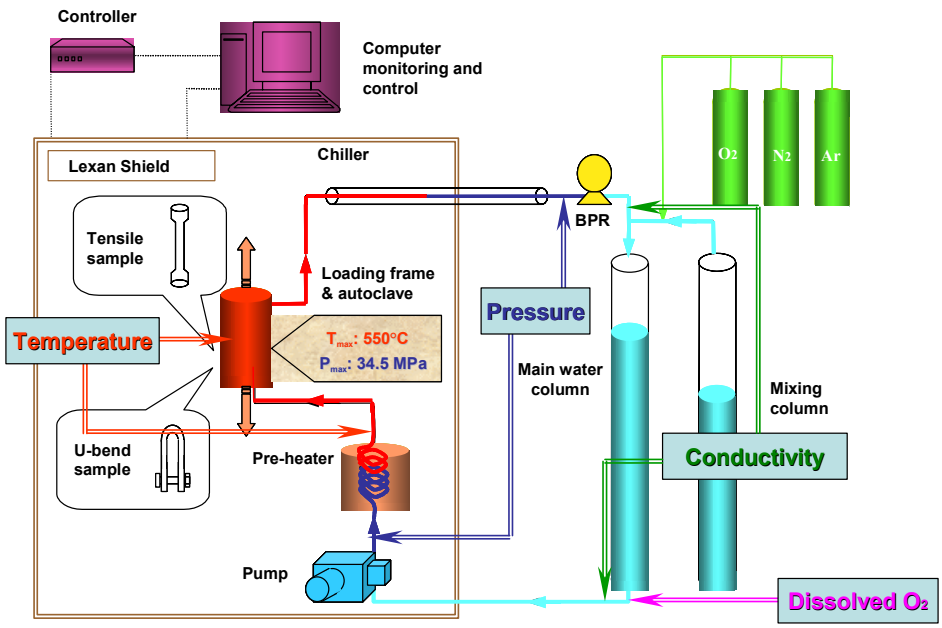

Figure 11. Schematic of the Supercritical water loop for stress corrosion cracking tests at the University of Michigan.

and outlet lines. Figures 12 and 13 show the overall view of the loop system and the load frame and loading elements.

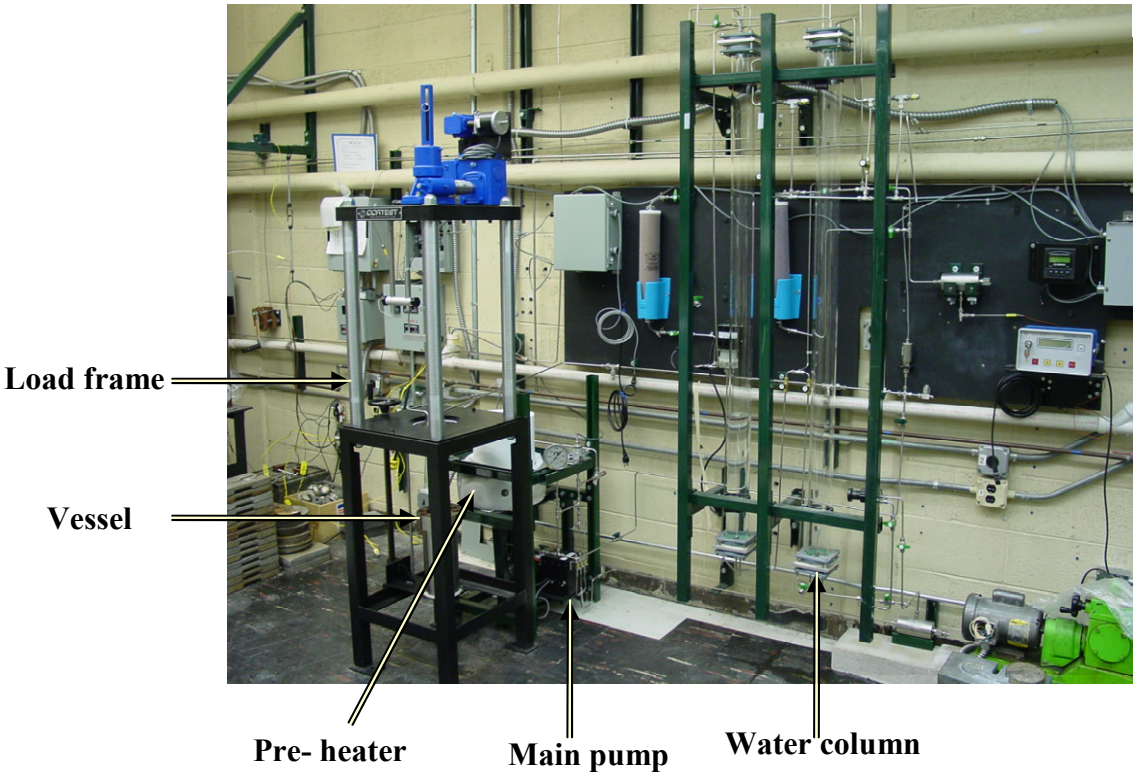

Figure 12. Overall view of the University of Michigan supercritical water loop system.

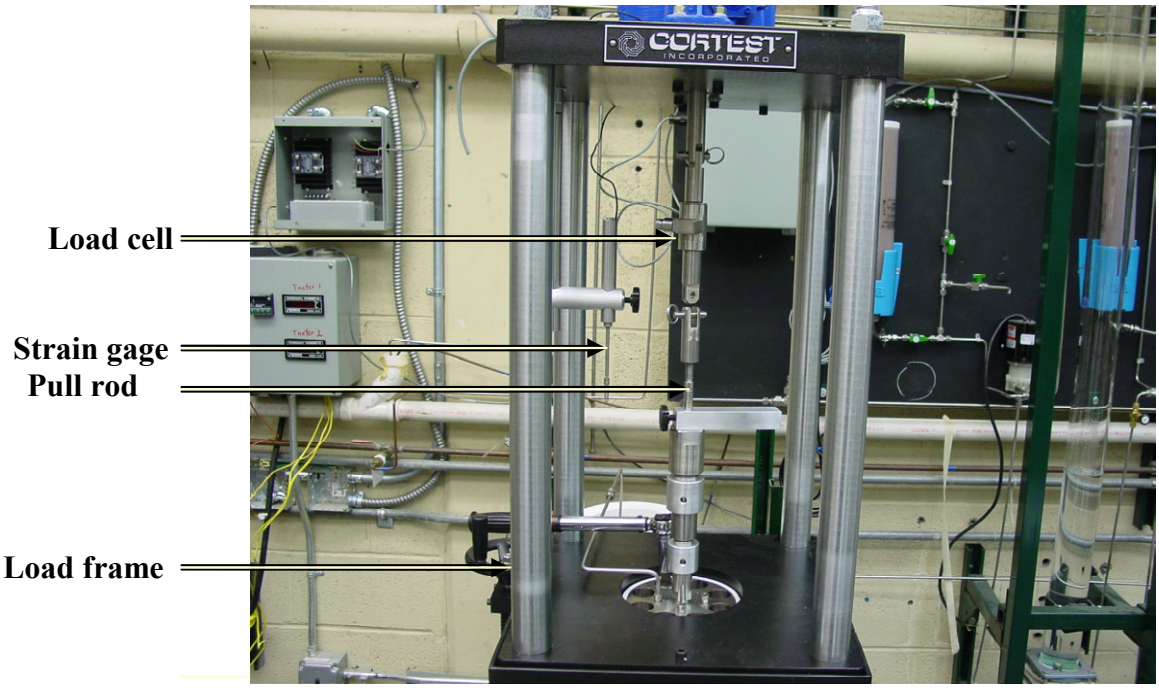

Figure 13. Supercritical water system: load frame and loading elements

During the 3rd quarter, the Supercritical Water Test Facility was evaluated. During this quarter, the main activity was to conduct a constant extension rate tensile test of commercial purity 304 at 550°C. This test will be described in Section 2.2.1 below. Some improvements concerning the safety and the reliability of the facility were implemented in the Supercritical Water Facility, and will be presented in section 2.2.2. The status of alloys for future experiments is given in section 2.2.3.

2.2.1. Stress Corrosion Cracking Behavior Of Alloy 304 In Supercritical Water

The section constitutes a review of the data collected during the first full constant extension rate test in supercritical water at 550°C. In the first part, the test sample and procedures will be presented. In the following three parts, the different phases of the test will be described, including; the ramp to the final pressure and temperature, the steady state period and the straining period. Results of the test are presented last. This section concludes with a description of recent modifications to the test apparatus and the status of the alloys planned for study in this program.

2.2.1.1. Description Of The Sample And Test Conditions

The sample used for the first test was a 304 stainless steel (Fe-18Cr-8Ni). The design of the sample is presented Figure 14. The same material had previously been tested under PWR and BWR conditions. The sample has a rectangular cross-section of approximately 1.9 mm in width and 1.3 mm in thickness, and was polished with SiC paper of successively increasing grade up to 4000. Then it was electropolished in a perchloric acid (10%) and methanol solution at -50 °C in two successive polishing cycles of 10 s each, at 30 V. The sample was cleaned with acetone and pure water before being installed in the vessel.

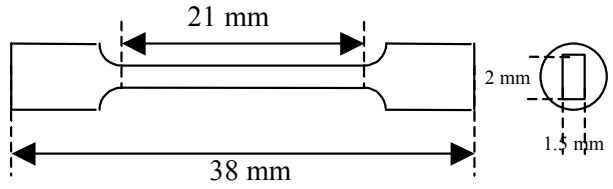

Figure 14. Constant extension rate test sample design.

The test conditions for the first SCW test were the following:

- Pressure: 25.5 MPa (3700 psig)
- Temperature: 550°C
- Environment: pure aerated water
    - Conductivity: the water conductivity was controlled at 0.06μS/cm both in the inlet and outlet line before the beginning of the test at high flow rate (50 ml/min). The conductivity was monitored during the experiment but as the conductivity values recorded are strongly flow rate dependant and the flow rate used during the test is 10 ml/min, the recorded values are more valuable as indications of the variation of conductivity and not as representative of the true conductivity.
    - Oxygen content: the values recorded at the beginning and at the end of the test were 6ppm
- Strain rate: 10^{-6} s^{-1} for the first 4% elongation and then 5x 10^{-7} s^{-1} until failure.

2.2.1.2. Ramp To Test Conditions:

The pressure was first increased up to 25.5MPa. Then the temperature was increased until 550°C. This operation required about 5 hours.

Figure 15 shows that the system pressure has two different types of behavior:

- Before 374 °C (transition temperature to the supercritical state), the variation range was around 40 psig (0.3 MPa). The increase in pressure corresponds to an increase in temperature, and when the temperature stabilized, the pressure recovered its initial value (see Figure 16). When the transition temperature of 374 °C is reached, the increase in pressure was higher (100 psig / 0.7 MPa).
- After 374 °C, the pressure variation range was around 20 psig (0.14 MPa), and is less strongly correlated with the increase of temperature.

Figure 17 shows the load recorded during the temperature increase. First, the load decreased from 0 lbs to -5 lbs between 20 °C and 374 °C in 3 steps (20 °C to 200°C, 200 °C to 250°C and 250 °C to 374 °C). Then, the load decreased to -85 lbs. The load recovered the value reached at 250 °C after 2 hours. During this recovery, the position recorded by the LVDT decreased at the rate of 50 µm per hour (see Figure 18).

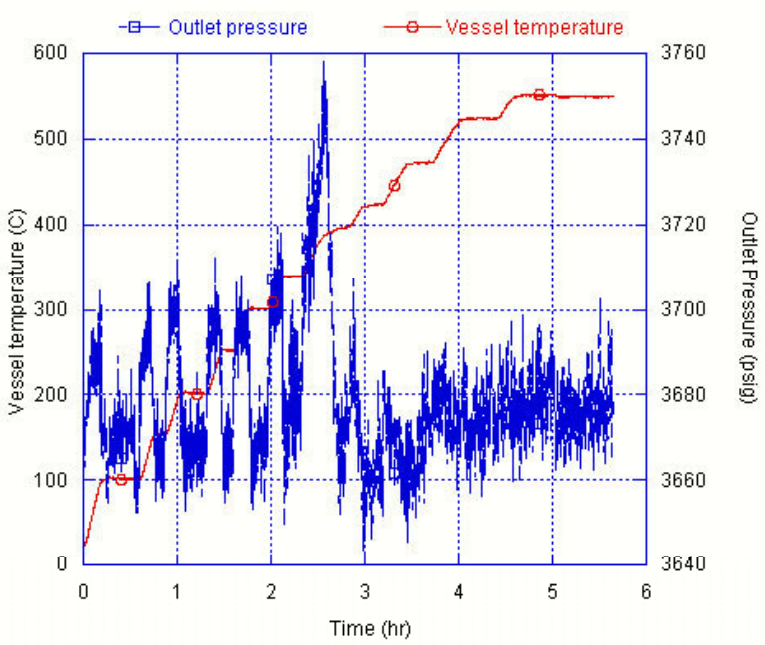

Figure 15. Evolution of the pressure and temperature during the temperature increase (before test conditions were achieved).

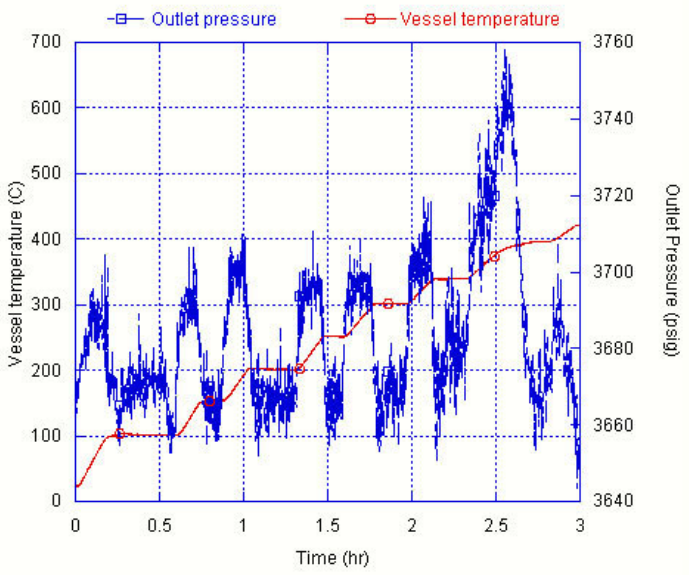

Figure 16. Evolution of the pressure and temperature before the supercritical temperature was achieved (0-3 hr time period from Figure 15).

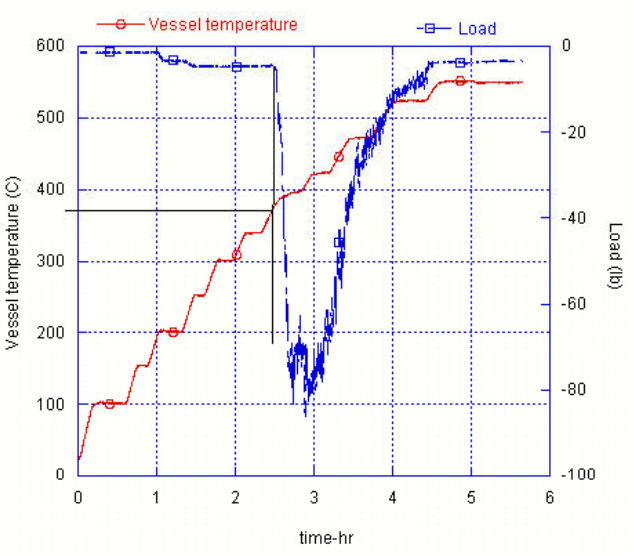

Figure 17. Evolution of the load during the temperature increase. When the transition temperature is reached, the load recorded drops of 80 lbs.

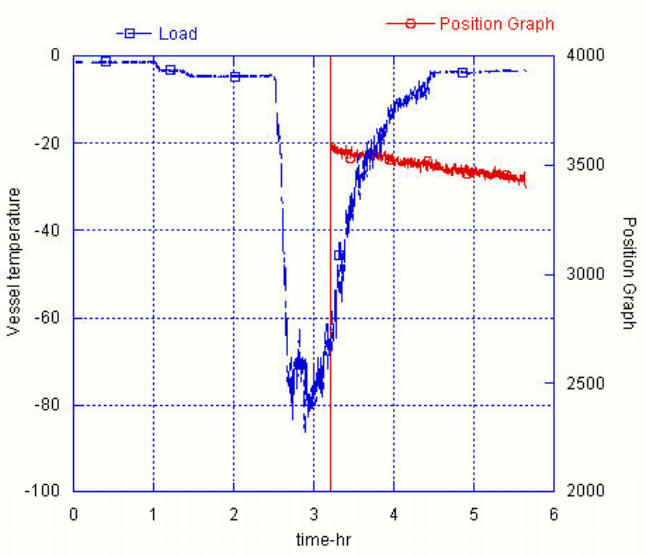

Figure 18. Evolution of the load and LVDT position during the temperature increase.

Figure 19 shows the evolution of the water conductivity in the inlet line (before the vessel) and in the outlet line (after the vessel). The water conductivity recorded in the inlet line increased from 0.3 to 0.4 µS/cm and then decreased to 0.3 µS/cm. In the outlet line, the conductivity increased from 0.1 to 2.2 µS/cm in two steps.

2.2.1.3. The Steady State Period

When the set points were reached, these conditions were maintained for a period of 16 hours to allow time to achieve steady state for all the parameters: pressure, temperature, load, position and conductivity. As shown in Figure 20, the pressure and temperature were stable during the steady state regime, with variations of ±20 psig (0.14 MPa) and ±1°C, respectively, over the 16 hour period.

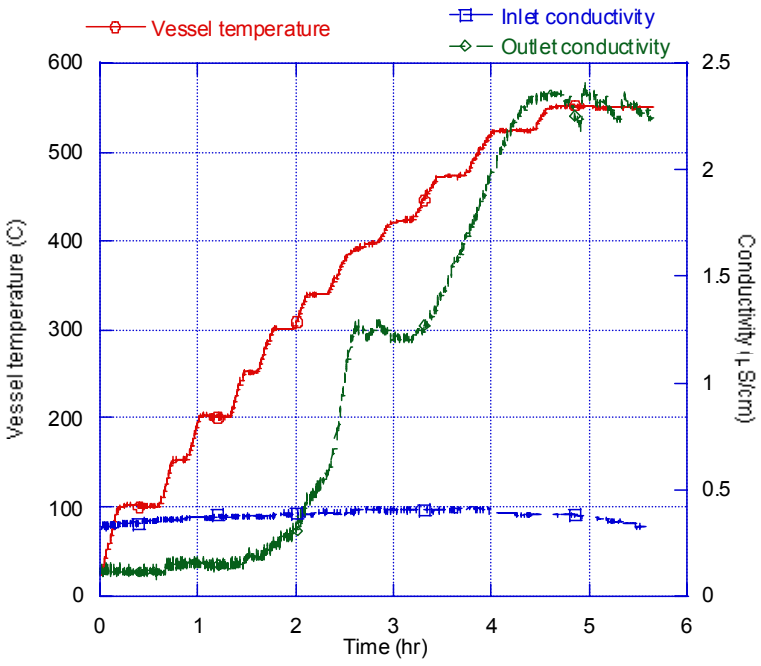

Figure 19. Evolution of the conductivity in the inlet and outlet lines during the temperature increase.

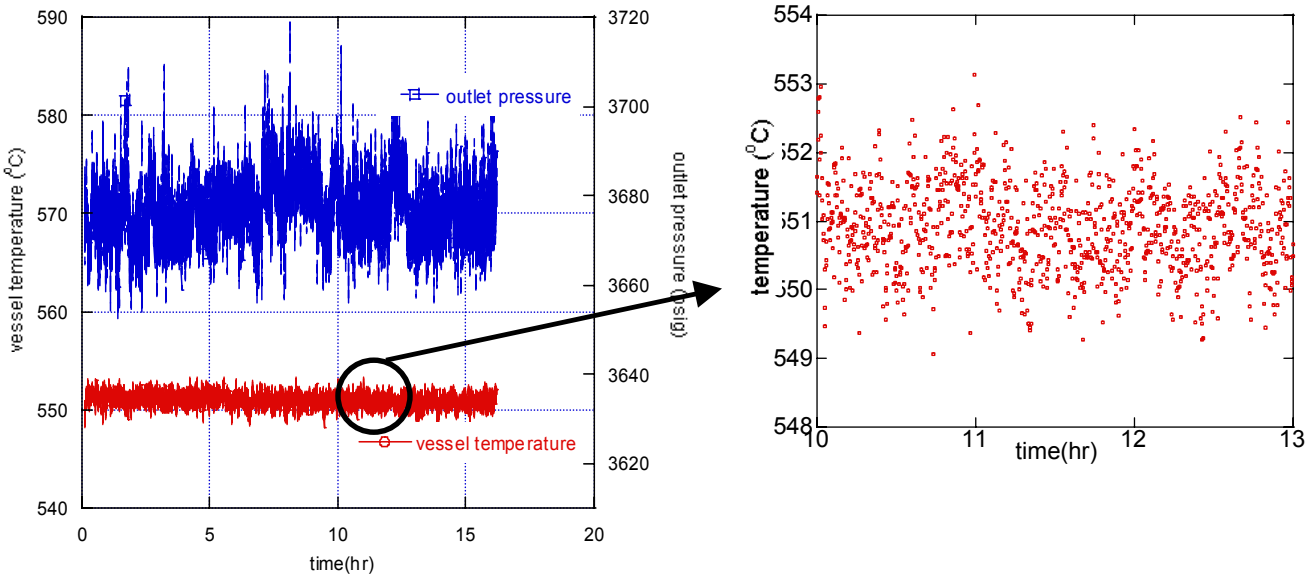

Figure 20. Pressure and temperature behavior during the steady state period .

As shown in Figure 21, the position, as determined from the LVDT measurement, continued to decrease following the trend described previously. But in 16 hours the position only decreased ~150 μm, or less than 10 μm/hr. The water conductivity recorded in both the inlet line and outlet lines, shown in Figure 22, decreased during this period. The inlet water conductivity dropped from 0.3 μS/cm to 0.25 μS/cm. In the same time, the outlet water conductivity dropped from 2.2 μS/cm to 1.2 μS/cm.

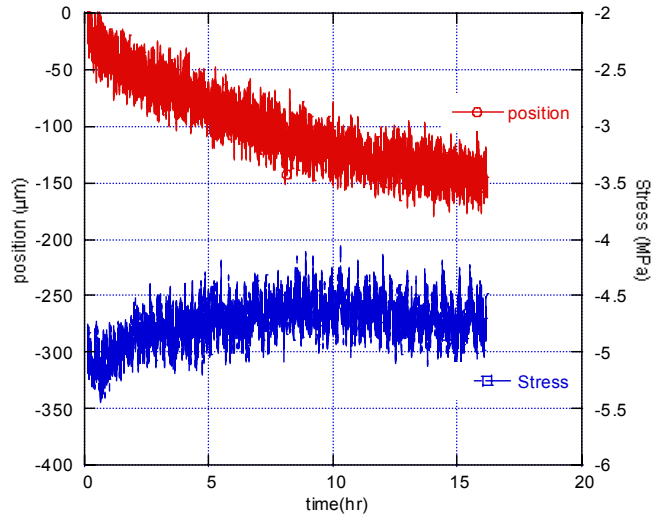

Figure 21. Position and stress variation during the steady state period.

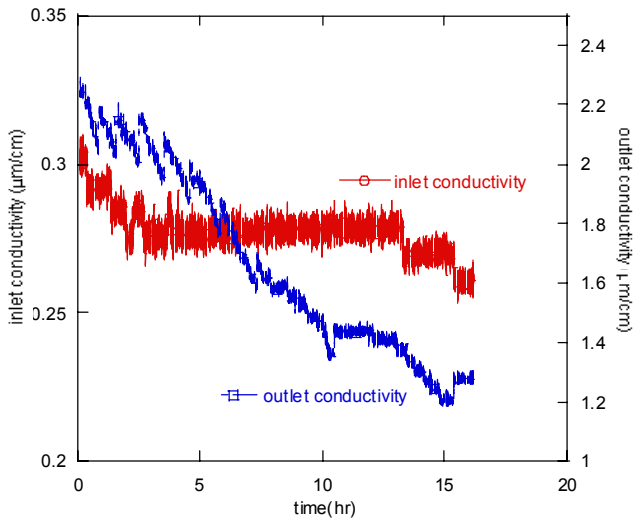

Figure 22. Conductivity recorded in the inlet line and in the outlet line during the steady state period.

2.2.1.4. System Behavior During Straining

Between the beginning and the end of the test, the pressure increased from 3680 psig (25.37 MPa) to 3720 (25.64 MPa). The pressure variation was around ±20 psig (0.14 MPa) (see Figure 23).

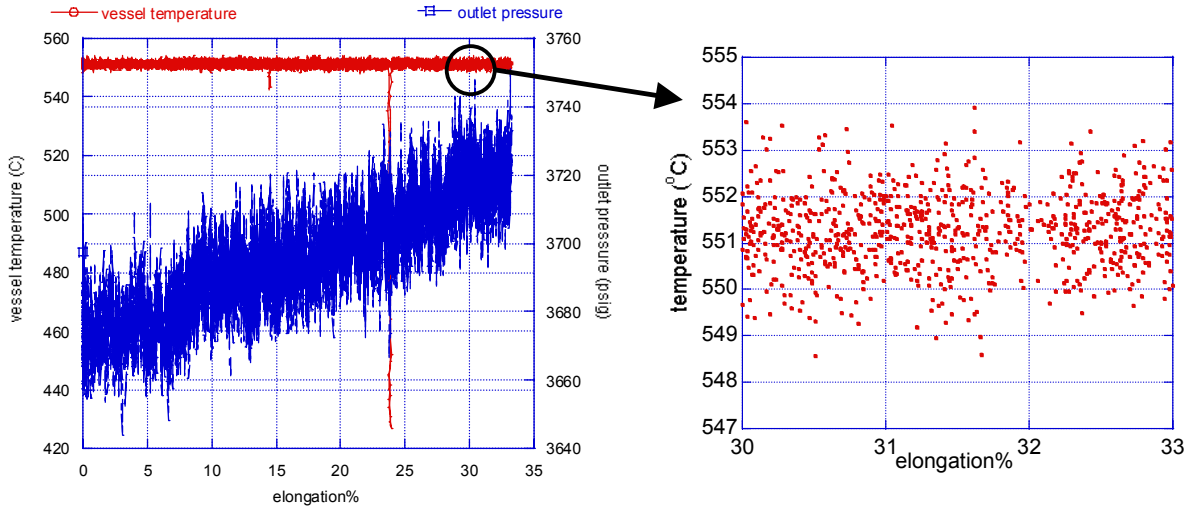

Figure 23. Temperature and pressure during the test.

The temperature was stable with a variation range around ±1 °C. A temperature drop appeared during the period of plastic deformation. This decrease of temperature was due to a local power loss. The temperature decreased by 120 °C, and the temperature was below the target temperature for about 1 hour, which corresponds to 0.2 % of elongation. The effect of this incident on the stress was a decrease of 60 MPa as shown in Figure 24.

The outlet conductivity continued to drop until it stabilized at 0.6 µS/cm, as shown in Figure 25.

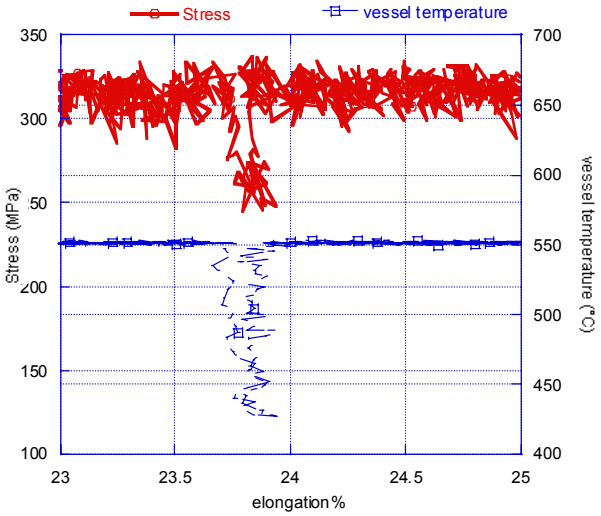

Figure 24. Decrease of the stress due to a drop in temperature.

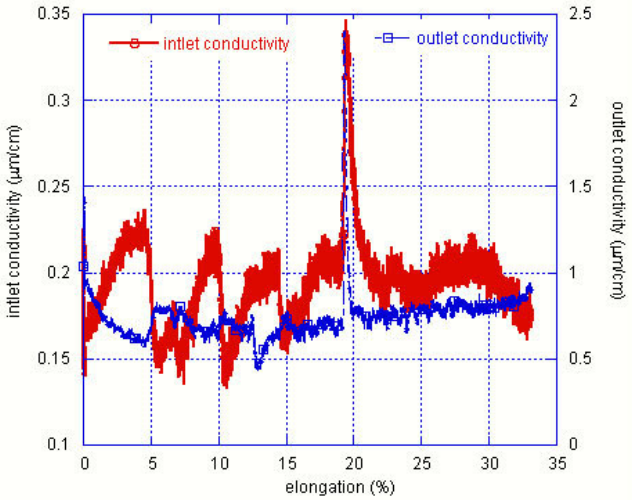

Figure 25. Evolution of the conductivity during the test.

The variation in sample position as measured by the LVDT was about ±8 µm. The total length of the sample after the test was 44.3 mm, which compared to the initial length of 38 mm, yielded a 6.3 mm elongation. This value is in good agreement with the 6.7 mm of elongation recorded by the LVDT during

the test. As shown in Figure 26, the variation in stress depended in the value of the stress. When the stress was around 300 MPa, the stress variation range was ± 20 MPa. Early in the test, at low stress, and after the sample failed, the variation of the stress was around ± 2 MPa.

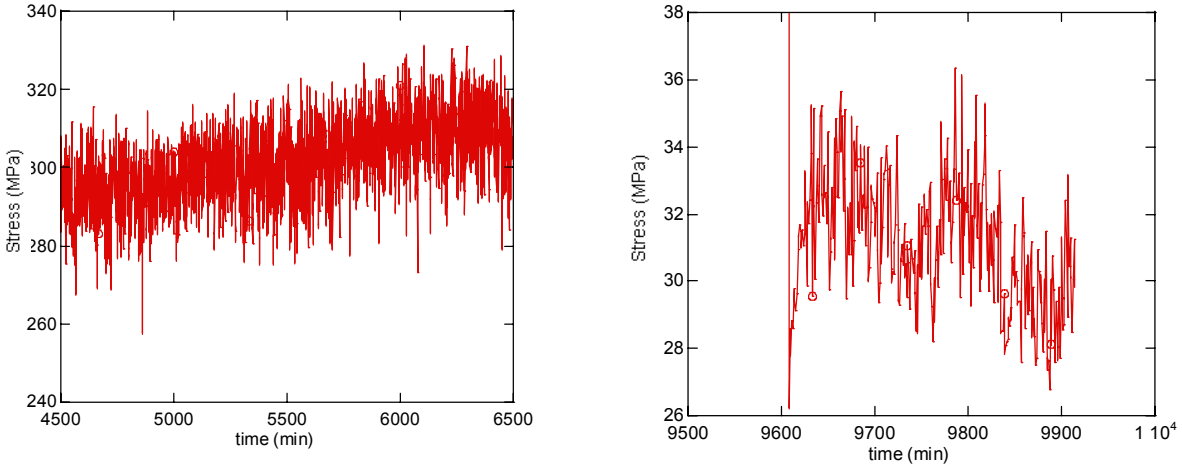

a) b)

Figure 26. Variation of stress during the test, a) high stress, and b) after sample failure. The variation range depends on the stress applied.

2.2.1.5. Test Results

The stress-strain curve is plotted in Figure 27. At the beginning of the test, the stress increased without any movement of the pull rod because of the static friction between the bal seals and the pull rod. Once the applied stress exceeded the friction stress, the pull rod started moving and the stress read by the load cell dropped to the value of the dynamic friction stress (Figure 28). Once the slack in the load train was eliminated, the sample began to strain.

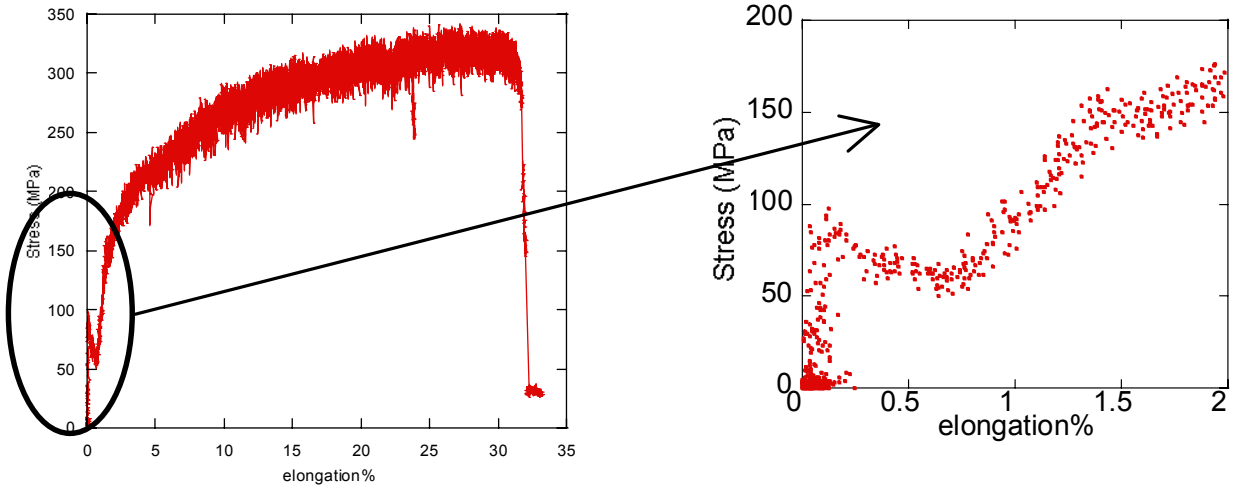

Figure 27. Stress-strain curve for commercial purity 304 stainless steel at 550°C and 25.5 MPa.

The stress on the sample is the recorded stress less the dynamic friction stress. As the dynamic friction stress is about 55 MPa, the stress on the sample is 55 MPa lower that the value recorded. The yield stress was reached at 100 MPa. The maximum stress is 280 MPa and rupture occurred after about 30% elongation. At the end of the test, the residual stress of 30 MPa recorded by the load cell is due to the dynamic friction stress (+55MPa) and the pressure applied on the half sample (-25.5 MPa).

2.2.1.6. Characterization of the cracks.

Necking of the cross section was minimal as shown in the micrograph in Figure 29. A large number of secondary cracks are visible on the side of the sample. The density of the cracks is around 20 crack/mm^2. Cracks also occured well away from the fracture region. At high magnification (Figure 30), the secondary cracks indicate that the surface fractures are intergranular.

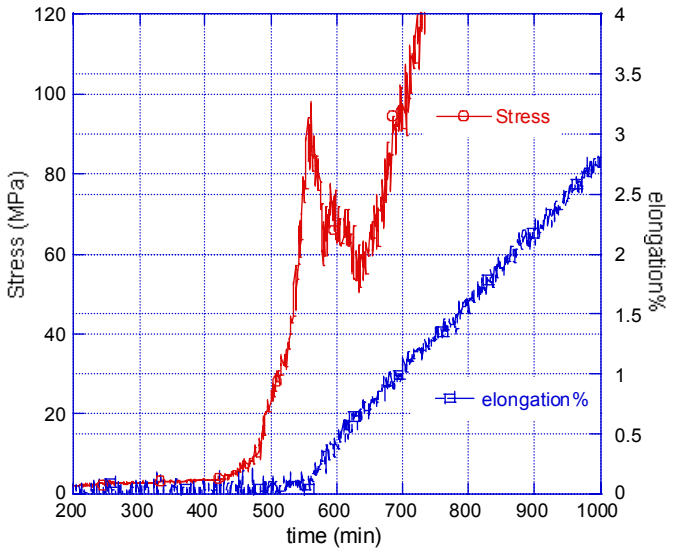

Figure 28. Stress and elongation versus time during the first few hours after the motor was started. The pull rod connected to the sample start moving after the static friction stress on the pull rod has been overcome.

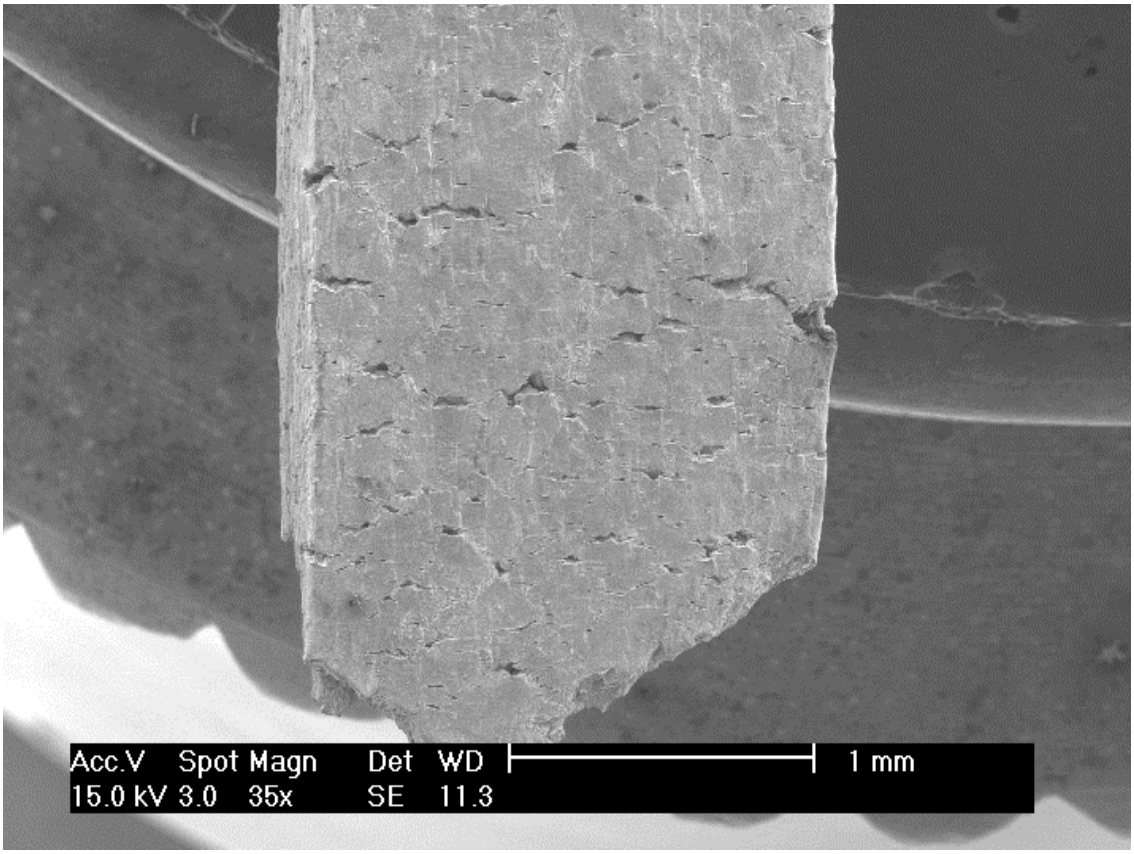

Figure 29. Sample surface after SCC test: secondary cracks appear all over the surface

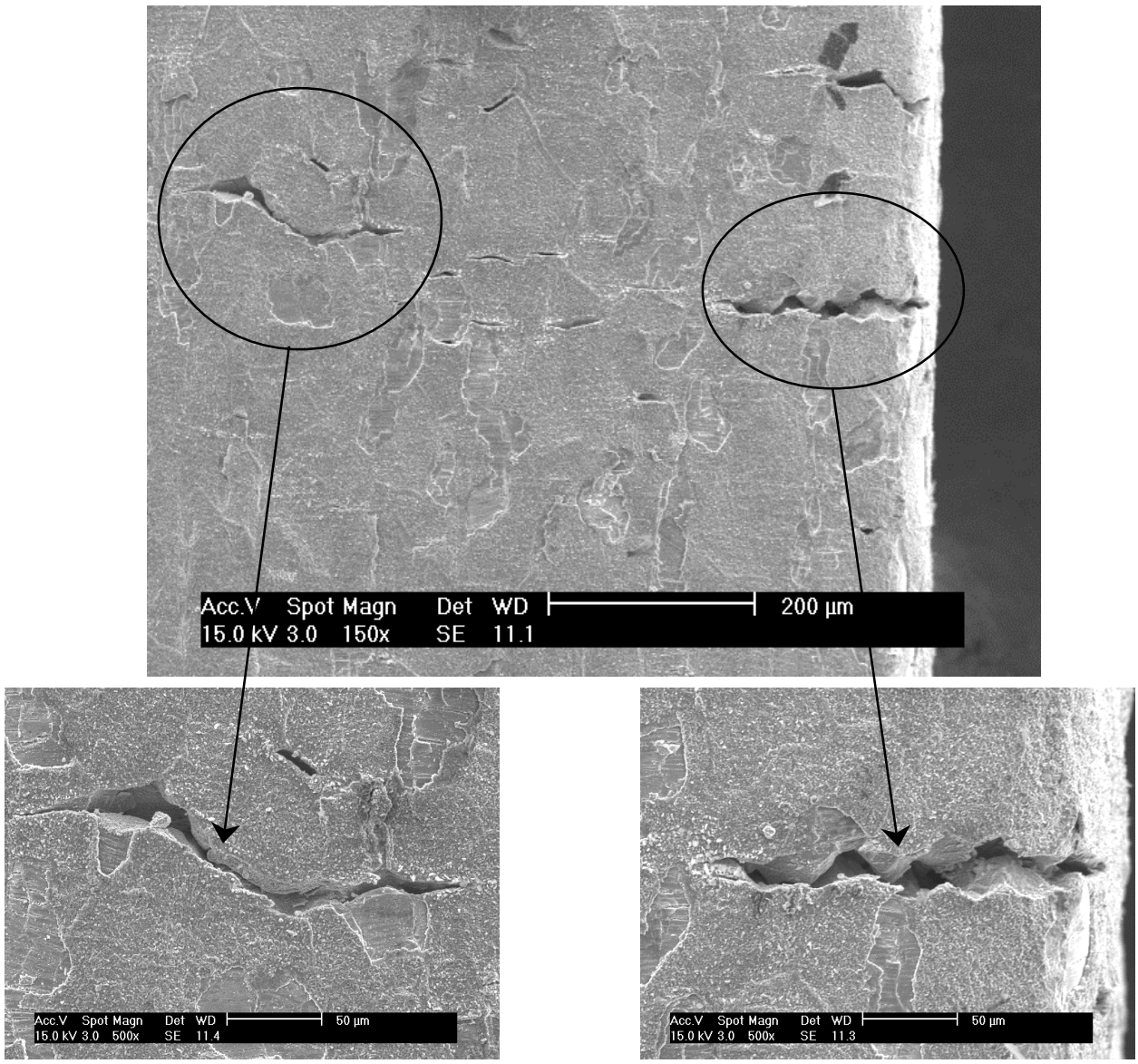

Figure 30. Cracks on the sample surface. The high magnification micrographs show the intergranular nature of the cracks.

Figure 31 shows the fracture surface of the sample. Intergranular fracture occurred in multiple locations as shown by the circled regions in Figure 31. The balance of the fracture surface is typical of ductile rupture indicating that failure occurred by ductile rupture, but was initiated by intergranular fracture. It should be noted that this same material has previously been tested under PWR and BWR conditions and the intergranular surface cracking shown in Figures 29, 30 amd 31 did not occur.

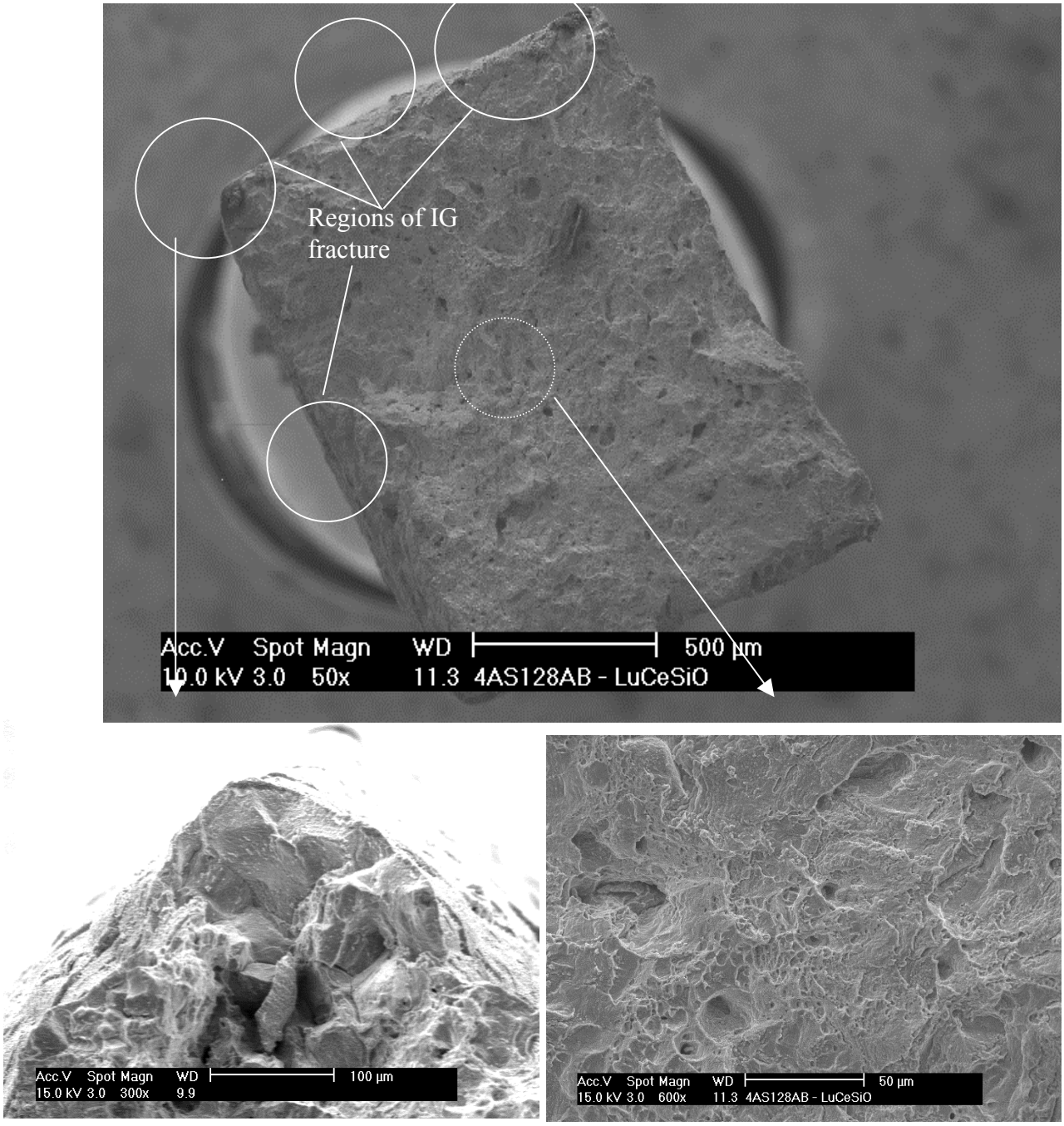

Figure 31. Fracture surface of CP 304 SS following straining in 550°C water to 31%. Regions of IG fracture are shown in the circles.

2.2.2. Modifications to the System

Several modifications to the supercritical water SCC test system have been implemented during this quarter. Two of these modifications increased the safety of the system. The other two improved the system's stability, reliability, and ease of use.

The third quarter report described a planned safety program to monitor the temperature and pressure of the experiment 24 hours a day. This program has been implemented and successfully tested. The computer-monitoring program sends a message to a pager whenever the pressure or temperature of the system exceeds a prescribed range. The experimenter receiving the page can then attend to whatever problem has occurred. Temperature limit controllers have also been installed as a backup to the pager system.

The two other modifications were a new temperature control system and an improved LabView control program interface. The old control system was based on an on-off logic for the heater, causing the heater bands to be either at full power or zero power. This made temperature control difficult and also shortened the life of the heating elements. A new temperature control system, based on analog proportional control logic, was obtained from a different company (Athena) and installed. The Athena temperature control system maintained a temperature control of ±1 °C once at temperature, and it was able to increase or decrease the temperature with little overshoot of the set point. The improved LabView interface increased the ease of reading the values for temperature, pressure, and conductivity. It also added the option of switching between plots of the various process variables being measured during a test.

The next step will be to improve the water conductivity meters system to be confident in there reading.

2.2.3. Alloys for the Supercritical Water Stress Corrosion Cracking Testing

Since the previous quarterly report, all of the alloys for the project have been ordered and received. Data on the seven alloys is summarized in Table 1. Alloy 693 was sent by Special Metals Corporation along with Alloys 625, 690, and 718. Alloy 693 has similar corrosion resistance properties to its predecessor Alloy 690, but the addition of aluminum to the alloy increases corrosion resistance to other phenomena, including metal dusting. The next step will be to conduct the final heat treatments in preparation for the first experiments.

Table 1. Summary of alloys obtained for future experiments.

Alloy	Sample Size Received (in.)	Description	Condition	Supplier	Date
316	0.5x6x12	Austenitic Stainless Steel	As-rolled	Metal Shorts Incorporated	8/15/02
HT9	0.375x4.5x10	3-phase: Martensite, Austenite, and δ-Ferrite	As-rolled	OAK Ridge Nat. Laboratory	9/05/02
T91	0.5x12.2x53.5	Martensitic Stainless Steel	As-rolled	American Alloy Steel	8/16/02
625	0.5x3x29	Precipitation Strengthened Ni-based Alloy	Hot-rolled, Annealed	Special Metals Corporation	9/12/02
690	05x3.2x4.6	Solid Solution Strengthened Ni-based Alloy	Hot-rolled, Annealed	Special Metals Corporation	9/12/02
693	5/16x6.5x12.4	Solid Solution Strengthened Ni-based Alloy	Hot-rolled, Annealed	Special Metals Corporation	9/12/02
718	11/16x3.25x20	Precipitation Strengthened Ni-based Alloy	Hot-rolled, Annealed	Special Metals Corporation	9/12/02

Task 3 Results: Plant Engineering and Reactor Safety Analysis (Dr. Luca Oriani, Westinghouse Electric Company)

3.1. Introduction

This section contains a summary and overview of the Westinghouse activities during Year 1 of this NERI project and information on how the work will be developed during the second year. Also, more detail on the activities performed during the fourth quarter is provided. In agreement with the original scope of the proposal and with the project direction given by INEEL, the focus of the project has been on identifying all the potential feasibility issues that the development of a supercritical light water reactor may pose.

The input for this section has been organized on a task basis: for sections where input has been already been provided, references to previous quarterlies are used, and only the principal results are reported. The nomenclature, subscripts, and acronyms for Section 3 are listed in Appendix A.

3.2. Conceptual Design of the Reactor Coolant System

The preliminary assessment of different plant concepts has been presented in the progress report for year 1, second quarter (MacDonald et al., 2002).

Different solutions proposed by other research groups have been considered (Oka and Koshizuka 2000 & 2001, Spinks et al. 2002, Heusner et al. 2000) and compared to the design of the most advanced PWR (Westinghouse AP600/AP1000, IRIS) and BWR (GE ESBWR) concepts. Both a direct cycle and an indirect cycle (loop design and integral layout) were considered: a conceptual layout of the different plant concepts is shown in Figure 32.

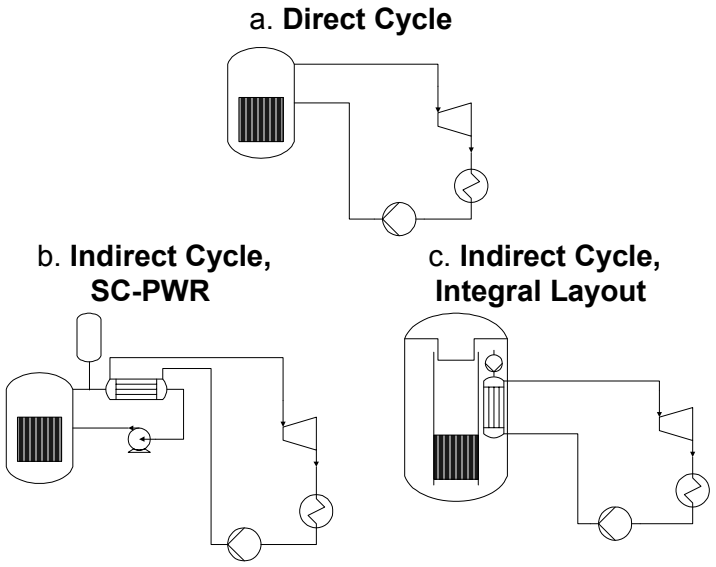

Figure 32. Different plant concepts for the Supercritical Light Water Reactor

For the preliminary studies, a direct cycle option that takes full advantage of the compact design and thermal hydraulic performance of the system was selected as the reference, even though other options are still considered in case future analyses should suggest that a different approach might be required. The reasons for selecting a direct cycle are:

1. The Direct cycle approach takes full advantage of the system characteristics: compared to a BWR, it allows a significant reduction in vessel size thanks to the adoption of a once-through configuration and the elimination of the steam separators and driers, recirculation loops and pumps, and jet pumps. The elimination of the steam separators and driers allows the adoption of PWR CRDMs (control rod drive mechanisms) that eliminate lower vessel penetrations and simplify the design compared to BWRs. Compared to a PWR, a direct cycle allows the elimination of all the components of a PWR primary loop (steam generator, reactor coolant pumps, pressurizer, and loop piping).

2. An integral primary-system layout indirect cycle is penalized by the large vessel dimensions that are intrinsic to this concept. Given the high pressure of the SCWR, this penalization is more important for the SCWR than for current operating conditions of PWRs.

3. A loop indirect cycle (similar to solutions studied in the past by Westinghouse) would be similar to present day PWRs, and the main feasibility issues would be connected to the design of the major primary system components (steam generator/heat exchangers, pressurizer, and coolant pumps) for the operating pressures and temperatures envisioned for the SCWR. The same reactor pressure vessel proposed for the direct cycle solution would be employed, so that several considerations and analysis that will be developed for the direct cycle option will be immediately applicable to the indirect cycle alternative. This solution will be considered as an alternative to the selected reference design, in case further studies and analyses should evidentiate any feasibility issues connected to the adoption of an indirect cycle.

The INEEL position, shared by Westinghouse, is to develop a design concept that relies on passive safety systems, similar to the more advanced plant concept currently being developed by the three main NSSS vendors: the AP600/AP1000 and IRIS (Westinghouse), the SBWR/ESBWR (GE) and the SWR-1000 (Framatome ANP).

The selection of a reference and backup solution for the plant concept allows an initial system conceptual layout. Current plant configuration and operation activities are discussed in Section 3.5, and a reference layout for the pressure vessel is presented.

3.3. Definition of Thermal/Mechanical Design Limits

The NRC fuel rod design criteria outlined in the Standard Review Plan were assessed against the SCWR operating characteristic in the progress reports for the second and third quarter (MacDonald et al., 2002) and only main results are summarized here.

A set of design criteria to replace the minimum departure from nucleate boiling ratio (MDNBR) and critical power ratio (CPR) used in PWR and BWR designs were defined on the basis of the fuel cladding temperature. Preliminary discussions with INEEL on the basis of material studies performed as part of this project and comparison with other SCWR development programs, led to the definition of a maximum allowable cladding temperature for ANSI Condition I (MAT-I) events of 620°C to preserve clad lifetime (for the Alloy 718 clad selected for this study). For ANSI condition II events (incident of moderated frequency), to prevent fuel rod damage due to overheating, a maximum allowable cladding temperature (MAT-II) of 840°C was defined. These values should be considered only as indicative and subject to

change as the design evolves and better information on the cladding behavior and characteristics in supercritical water conditions are collected.

Due to the higher coolant/cladding temperature, some preliminary analyses were devoted to evaluate the power-to-melt for the SCWR and thus identify eventual limits to the core linear power. The INEEL estimated the power to melt using the FRAPCON code, assuming a cladding temperature of 840°C for Condition II events. The calculated power-to-melt was 54.6 KW/m. This result still needs to be confirmed and a more thorough investigation will be performed at the INEEL and Westinghouse in the next quarter.

The initial results obtained with a simplified thermal-hydraulic analyses of the SCWR core confirmed the critical importance of the hot channel factors due to the very large enthalpy rise in the core (the enthalpy rise in the SCWR is an order of magnitude larger than PWRs and BWRs). These analyses have been discussed in detail in the third quarter progress report (MacDonald et al. 2002), and are summarized in Section 3.4.2.

3.4. Core Thermal-Hydraulic Design

The INEEL is responsible for the core neutronic design of the SCWR, and several options have been considered during the first year activities. A reference fuel assembly design was defined, with results presented in the progress report for the third quarter (MacDonald et al. 2002). Activities have proceeded during the fourth quarter, and a preliminary core design and an updated assembly design are presented in Section 1 above. The fuel assembly design and main assembly data are summarized in Figure 33. The design proposed for the SCWR features cruciform control rods around each fuel assembly. A fuel assembly consists of a rod/moderator bundle (19x19) and the channel that surrounds it.

The choice of cruciform control rods was suggested by INEEL for preliminary core design because they can be accommodated in the relatively wide inter-assembly gap that was necessary for more uniform moderation of the peripheral rods. Other solutions (PWR rodlets, either occupying fuel rod lattice positions or inside the moderator boxes) are considered as alternatives.

The fuel rod and assembly data used by INEEL in their preliminary analyses were reviewed and discussed by Westinghouse and INEEL and based on Westinghouse experience and

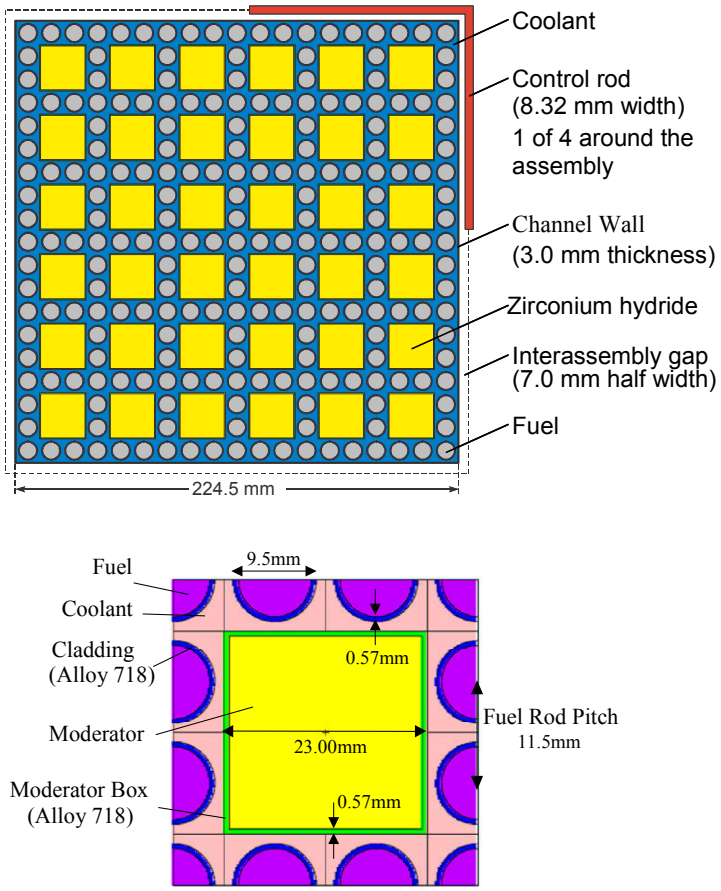

Figure 33. Fuel assembly (and fuel cell detail) with updated data.

comparison with both PWR (Westinghouse) and BWR (GE, Westinghouse-Atom) data, the reference assembly design (Figures 2 and 5) was adjusted slightly as shown in Figure 33. The neutronic results presented in this report were obtained by the INEEL with the dimensions shown in Figures 2 and 5, and will be updated in the future with these new data. However, little or no change in the results presented in Section 1 is expected.

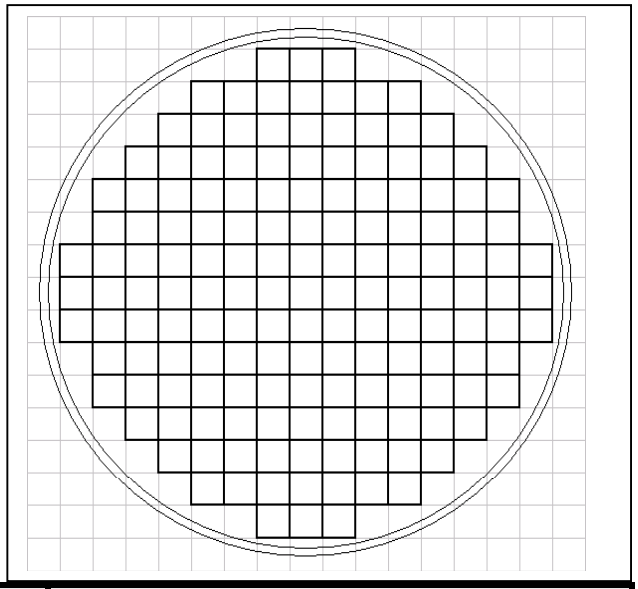

A 157-assembly core has been selected as the reference core design. The core layout, typical of Westinghouse 3-Loop plants and of the AP1000 is shown in Figure 34. Table 2 summarizes the main assembly and core dimensions for use in the analyses.

Table 2 – Main Assembly and Core Data

FUEL ASSEMBLY		CORE	
Fuel Rod			
Rod OD/ID [mm]	9.50/8.36	Number of Assemblies	157
Cladding Thickness [mm]	0.57	Thermal Power [MWt]	2700
Pellet OD [mm]	8.19	Average Linear Power [KW/m]	18.56
Active Length [mm]	4270	Power per Rod [KW]	79.25
Rod Pitch [mm]	11.50	Power per Assembly [MW]	17.206
Moderator Box		Core Power Density [KW/l]	70.8
Box side [mm]	23.00	Core Equivalent Diameter [mm]	3372
Cladding Thickness [mm]	0.57	**Barrel Dimensions**	
Assembly Channel		Core Barrel ID [mm]	3800
Channel Wall Thickness [mm]	3.00	Core Barrel OD [mm]	3900
Channel Side [mm]	224.5		
Cruciform Control Rods			
Thickness [mm]	8.32		
Fuel Assembly			
Interassembly Gap [mm]	14.0		
Assembly Pitch [mm]	238.5		
Fuel Rod per Assembly	217		
Moderator Boxes per Assembly	36		
Fraction of Lattice Positions available for Fuel Rods	60.11%		

A core power of 2700 MWt has been selected for this reference core, giving a linear power similar to that of advanced PWRs (18.56 KW/m). The calculated core power density (70.8 KW/l) is somewhat halfway between that of a PWR (100+ KW/l) and that of a BWR (50-55 KW/l). Although this 157-assembly core has been defined as reference for preliminary design studies, a 193-fuel element core (Westinghouse 4-Loop Plants) with about 3300 MWt is considered as a reasonable alternative. The final choice between the two plant sizes will be based on the design of the passive safety system configuration and the system

response to different design basis accidents. Also, the possibility of reducing linear power will be considered based on the results of the preliminary analyses.

It must be stressed that the assembly and core design are only indicative of a possible design, and this information is provided only to allow initial system evaluation, and should not be considered as a "real" design proposal.

3.4.1. Preliminary Thermal Hydraulic Analyses - Evaluation Models

One of the first tasks performed by both the INEEL and Westinghouse during the first year was devoted to the assessment of the available tools for the analysis of a SCWR. The deficiencies in the currently available codes and models can be essentially grouped into two main areas:

1. Constitutive models and physical properties for SCWR analyses. Appropriate heat transfer correlations for SCWRs are needed. An extensive assessment of the available heat transfer correlations was presented in the third quarter progress report. We discussed precedent studies by European (Cheng and Shulenberg 2002) and Japanese research groups and developed an additional, more in depth assessment of two of the most promising correlations (the Bishop and Oka-Koshizuka correlations). The overall conclusion is that although both correlations might be used for preliminary analyses since they present acceptable results, an extensive effort will have to be developed to define heat transfer correlations for supercritical water, especially considering the complex geometries typical of a fuel bundle.

2. Computer Codes for the analyses of SCWRs. The INEEL has modifyed the RELAP 3D computer code and plans to use it as the system code for transient and accident analyses of SCWRs. INEEL/Westinghouse recently requested a waiver from DOE to allow the use of proprietary Westinghouse codes in performing subchannel analyses on the SCWR. Thanks to this waiver, the W-VIPRE code will be used for subchannel analyses on the SCWR. A more detailed discussion of the codes and their adaptability to SCWR studies is given below.

This initial assessment phase, that is still to be completed in the area of code development, allows the definition of a sufficient set of tools (computational tools and constitutive models) to perform initial analyses on the SCWR, while parallel activities will have to be continued (especially in the area of heat transfer in supercritical water) to develop more appropriate tools.

3.4.1.1. System Analysis - RELAP 3D

The RELAP 3D code has been identified by INEEL as the system code for SCWR studies and will be used to describe the nuclear steam supply system and the engineered safeguard features of the reactor. The INEEL has extensive experience with the development of this code, and already implemented modifications to the code for its application to SCWRs. These modifications are discussed in the previous two quarterly reports. An input deck for the SCWR concept described in Sections 3.2 and 3.5 is under development and will be used to perform preliminary analyses and improve the understanding of the SCWR operational characteristic and safety related features.

3.4.1.2. Core Thermal-Hydraulic Analysis – W-VIPRE

Westinghouse has recently received from DOE a waiver that allows the use of proprietary codes for the SCWR analyses. Thanks to this waiver and DOE support, Westinghouse plans on using the W-VIPRE code for the subchannel analyses of the SCWR. W-VIPRE is the Westinghouse version of VIPRE-01

computer code (Stewart 1989), a three-dimensional subchannel analysis code that has been developed to account for hydraulic and nuclear effects on the enthalpy rise in the core and hot channels. VIPRE-W modeling of a PWR core is based on a one-pass modeling approach. In one-pass modeling, hot channels and their adjacent channels are modeled in detail, while the rest of the core is modeled simultaneously with a relatively coarse mesh. A similar approach will be used to model the supercritical water core.

To adapt the code to SCWR a three-step program has been adopted:

1. Assess the code capability in modeling, and analyze the SCWR on the basis of Westinghouse in-house experience with the code.
2. Develop the code modifications necessary to apply the code to SCWRs and identify appropriate evaluation models and assumptions for core analyses.
3. Develop two core models for the study of (a) orificing and overall core behavior and (b) calculation of peak cladding temperature for different operational, abnormal, and accident scenarios.

The first step has been already completed, and the results are discussed in the following sections. This initial assessment is adequate to identify the effort that will be necessary to complete Step 2. It is currently estimated that Step 2 will be completed in the first quarter of Year 2 of this project, at least in a preliminary way. Model development and preparation of the two input decks has been already initiated, using the core reference design defined in the previous sections.

3.4.1.3. Initial Assessment of the W-VIPRE Computer Code for SCWR Analyses

The VIPRE family of codes has been extensively used both for PWR and BWR studies. Moreover, the VIPRE-01 validation includes some analysis of supercritical pressure transients to verify the code capabilities in following a large pressure excursion transient. Westinghouse has extensive experience in the use of the code, and uses it for both safety analyses and core thermal hydraulic design. A preliminary assessment of the code has been completed to identify potential issues that might require additional development effort before the code can be successfully applied to SCWR analyses. This assessment can only be considered preliminary, as more issues will probably be identified as the code is used in SCWR analyses.

The VIPRE input deck can be divided in several different input groups, which are discussed here in some detail:

- **Core Geometry**. The geometry proposed by the INEEL for the SCWR core has several features in common with that of BWR/PWR cores, but presents the complication of the solid moderator boxes. Modeling of the square moderator box is not possible with VIPRE without modifications to the code. However, the moderator box modeling is not considered fundamental at this stage of the analyses: only the effect on the subchannel wetted perimeter will be accounted for, and in this core model it will be assumed that 97.5% of the power is generated in the fuel rods and the remaining 2.5% is generated in the coolant. Separate analyses will be developed on the moderator box to calculate temperature profiles and other performance parameters.

- **Water Properties**. VIPRE calculates fluid properties as a function of fluid pressure and enthalpy either by extracting the properties from a table or by computing the properties directly from curve fit functions. These functions were developed by EPRI for the RETRAN-02 code. The EPRI functions are valid in the range of 0.1 to 6000 psia (about 41 MPa) and 200 to 1750 Btu/lbm (about 4000 kJ/kg), which at 25 MPa corresponds to a temperature of 784°C. The range of these functions is not sufficient for SCWR studies (where cladding temperature limit for accidents of more than 800°C is

foreseen), and therefore user defined input properties will be used. Some care must be used in VIPRE when fluid properties are defined by the user, and a discussion on the chosen properties and proper input definition will be part of the model development (to be completed during the second year).

- **Nuclear Rods**. The fuel rod geometry is similar to that used in Westinghouse PWRs, and no issue connected to the use of the VIPRE code is foreseen. Axial and radial power profiles will be input according to results obtained by the INEEL. It is important to note that both in PWR and BWR analyses the radial and axial power shapes used in subchannel analyses are not based on best estimate calculations, but rather assume some limit values and shapes to bound all possible operating and abnormal conditions. Some care must therefore be used in implementing the power profiles in the input decks for core analysis if meaningful results are to be obtained. The fuel pellet modeling does not present significant differences from common Westinghouse experience. VIPRE allows the user to define cladding and fuel properties. The properties for Alloy 718 defined by other research groups that are part of this NERI program will be used in the analyses.

- **Operating conditions**. No issue foreseen. Conventional PWR and BWR methodology will be used to define core inlet parameters. For the transient analysis, the output of the RELAP code (for core pressure, inlet temperature, flow rate, and neutronic power) will be used to define the boundary conditions for the VIPRE model, that will then be used to perform transient core thermal hydraulic analysis.

- **Correlations (Heat Transfer and Friction)**. This is the part of the code that will require more extensive manipulation. First, both the Oka-Koshizuka and Bishop correlations will be implemented in the code to allow evaluation of heat transfer in supercritical water. Second, all the two-phase models (for two-phase friction multiplier, subcooled boiling, critical heat flux, and post-CHF heat transfer) will be disabled. Most of these modifications can be made by manipulating the input deck, and will not require extensive code review.

  For the axial friction loss coefficients Cheng (Cheng and Shulenberg 2002) suggest the use of a correlation developed by former Soviet Union researchers (Petrov and Popov 1988):

$$f = f_0 \cdot \left(\frac{\rho_w}{\rho_b} \right)^{0.4} \quad where \;\; f_0 = \left(1.82 \cdot \ln\left(\frac{\mathrm{Re}}{8} \right) \right)^{-0.2}$$

  VIPRE however allows the user only to define friction correlations in the form:

$$f = A \cdot RE^B + C$$

  where A, B and C are user defined constants. Two different options are available to model the proposed correlation: either the code is modified or the correlation is approximated using a VIPRE compatible function. One solution favors calculation precision, while the second favors simplicity of application. Both approaches will be evaluated and results compared.

  The cross-flow resistance between the different subchannels will use standard VIPRE procedures. The gap width and distance between channels will be defined according to common PWR and BWR practice. Resistance coefficients will be evaluated using typical PWR correlations for cross-flow over a bank of tubes. The geometry of the SCWR channel is different from that of a PWR core due to the presence of the moderator boxes, but the use of standard PWR models is considered acceptable as VIPRE is generally not very sensitive to the specific value of the crossflow resistance. Sensitivity

studies will be performed to quantify the potential error connected to the adoption of this simplified approach.

Loss coefficients for grids and grid positions will be defined for the model on the basis of Westinghouse experience and through the use of simplified correlations.

- **Turbulent Mixing**. The VIPRE energy and momentum equations contain terms describing the exchange of energy and momentum between adjacent channels due to turbulent mixing. This is not strictly a turbulent model, it is merely an attempt to account empirically for the effect of turbulent mixing. In many cases the contribution of turbulent mixing can be neglected, so the use of this option in VIPRE is optional. Vipre calculates turbulent cross-flow mixing between two channels connected by a gap using an equation in the form:

$$w' = ABETA \cdot S \cdot \overline{G}$$

Where w' is the turbulent cross-flow mass flow rate, ABETA is a user-defined coefficient, S is the gap width and $\overline{G}$ is the average mass velocity in the channels. Typical values for ABETA are between 0.003 and 0.004 for PWRs. A value of 0.004 will be used, and sensitivity studies will be performed to verify the impact of this assumption. Other input to this section will not require any deviation from common practice.

- **Program Execution Parameters.** No issue connected to the adoption of one of the various VIPRE solutions methods in anticipated. Based on results of preliminary analyses, the different solution schemes will be evaluated.

3.4.1.4. WVIPRE Model of the SCWR code

In parallel with the initial code assessment, preliminary input decks for VIPRE were prepared to describe the core geometry described in Figures 33 and 34. Two different input decks will be prepared for core analyses:

1. A quarter core model, with one computational channel per assembly. This model will be used to study/optimize orificing for the core and identify the location of the hot assembly. Also, the effects of various bypass terms will be evaluated.
2. A quarter core model, with the hot assembly modeled with one subchannel per rod and the rest of the core lumped in a small number of large channels. This model will be used to study the details of the hot assembly (including application of appropriate hot channel factors), calculating cladding and fuel temperatures and thermal-hydraulic characteristics of the channels. This model will be used to assure that the maximum allowable cladding temperature is not exceeded during Condition I and II events.

3.4.2. Preliminary Core Analysis and Assessment

In parallel with this initial activity aimed at developing a sufficient set of tools for the evaluation of the SCWR and, in particular, to identify areas where extensive experimental activity will be required, a preliminary assessment of the concept was performed to identify potential feasibility issues on which to focus activities during the second and third year. As far as core thermal hydraulic design is concerned, the main feasibility issue connected to the SCWR concept is the large enthalpy rise in the core. Figure 35 compares the SCWR (assuming an inlet core temperature of 280°C and a core outlet temperature of 510°C) with the AP1000 and the ABWR.

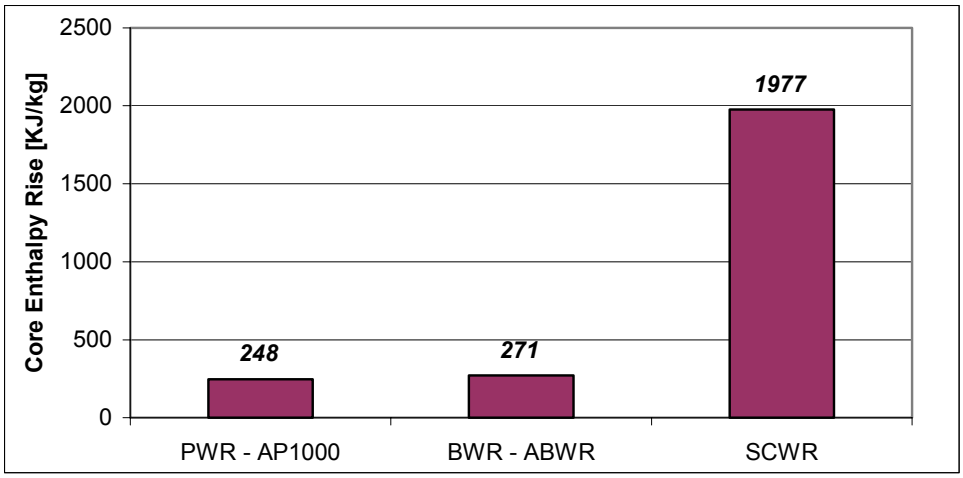

Figure 35 Core Enthalpy rise for different reactor concepts

Pages 61 to 63 of the third quarterly report (MacDonald, 2002) contain preliminary analyses of the SCWR that show the effects of the large enthalpy rise on the hot channel temperatures in a SCWR. The hot channel factors for the SCWR were defined on the basis of Westinghouse experience with PWRs. The following issues were identified on the basis of these initial results, and following discussions between INEEL and Westinghouse staff:

1. The SCWR is more sensitive than both PWRs and BWRs to hot channel uncertainty factors, it is especially sensitive to the hot channel uncertainty factors that affect the core enthalpy rise. A typical value of 1.3 for the hot channel enthalpy rise factor would lead to an increase in enthalpy rise of 30%, but to a much larger increase in core temperature: analyses presented in the first quarter showed an increase in the core outlet temperature between the average and the hot channel from 510 to 702°C. An appropriate treatment of the uncertainties, and, above all, a design that minimizes the hot channel uncertainty factors is required. A significant effort will be developed during Year 2 of this project to identify means of reducing the hot channel uncertainty factors.

2. For the same reason, achieving a flat radial power profile and also a flat local power profile is essential. Preliminary analyses developed by both the INEEL and other SCWR research groups are promising, showing relatively flat power profiles. It can be expected that the SCWR radial profile for the core design proposed by INEEL will be comparable to, or better than, those of advanced BWRs. It must be stressed that for both BWRs and PWRs the radial peaking factors used in thermal hydraulic analyses are conservative, and bound all the anticipated operating and abnormal conditions expected for the plant. The same care should be taken in SCWR studies, to guarantee that a fair and meaningful analysis is performed. The power profiles to be used in the thermal hydraulic analyses (both safety and design) will be jointly defined by the INEEL (on the basis of best estimate calculations) and Westinghouse (on the basis of common industry experience) staff.

3. To minimize the effect of the radial peaking factors, the adoption of canned assemblies and the development of an appropriate orificing scheme have been proposed and selected as our reference for further analyses. Also, to allow for sufficient design space, the system design temperatures have been modified to 280°C for the vessel inlet temperature 450°C for the vessel exit temperature. Based on the results of the analyses, the possibility for increasing the temperature will then be assessed.

4. The large enthalpy rise also requires that the core bypass flow is minimized. Assuming a core inlet temperature of 280°C (H=1230 kJ/kg), a core outlet temperature of 450°C (H=2951 kJ/kg), a system pressure of 25 bar and a typical (for advanced PWR) bypass rate of 6%, the vessel outlet temperature will be:

$$H_{vessel,out} = 2951 \cdot 0.94 + 1230 \cdot 0.06 = 2847.74$$

That corresponds to a vessel outlet temperature of ~432°C. Therefore, to maximize the system performance the core must be designed so as to minimize bypass flow rate. For preliminary analyses a bypass rate of 6% will be assumed, with a vessel outlet temperature of 450°C, and therefore a core outlet temperature of 474°C.

As evident from the previous considerations and from the simplified analyses performed in the previous quarterly, the large enthalpy rise and the connected issues have been identified as serious feasibility issues for the design of a SCWR core. For this reason, a large part of the activities in the future months will be devoted to assess these issues and identify possible solutions.

3.5. Plant Configuration and Conceptual Design of Required Safety Systems

During the final quarter of the first year Westinghouse initiated with INEEL activities in the area of system design. The scope of this first effort is to provide a reference design that can be used to perform transient and accident analyses using a RELAP nodalization that will be prepared by INEEL. The analyses will then be used to expand and complete the reference design on the basis of how the system will respond to different conditions.

INEEL and Westinghouse have agreed to a program for the development of a comprehensive plant design that will evolve along two different approaches:

1. **Task 3.5 and propaedeutic to Task 3.6.** A fuel assembly, core, and pressure vessel design is defined by INEEL (assembly design) and Westinghouse (assembly, core, and pressure vessel design). The assembly and core design have been discussed in previous sections, and the results summarized in Table 2 and Figures 33 and 34. A preliminary vessel design has been defined by Westinghouse and is described in Section 3.5.1 below. The INEEL staff will now develop a RELAP input deck of the proposed system design, while Westinghouse will develop a core model for subchannel analysis with the VIPRE code. The models will then be used to perform a preliminary assessment of the SCWR and evaluate the system inherent features: simple-forcing functions will be applied to the system, and the response will be evaluated. This assessment will be used to identify the main features, both positive and negative, of the system.

   A parallel qualitative assessment of the SCWR will be made by comparing the SCWR with the FSARs (Final Safety Analyses Reports) for different BWRs (mainly the BWR/6 Grand Gulf) and PWRs (Sequoyah and the AP1000). The adoption of a direct cycle system makes the SCWR more similar to a BWR from a safety point of view. The most important events for each of the USNRC Standard Review Plan (SRP) categories (decrease in reactor coolant temperature, increase in reactor pressure, decrease in reactor coolant flow, reactivity and power distribution anomalies, increase in reactor coolant inventory, decrease in reactor coolant inventory, radioactive release from subsystems and components, anticipated transients without SCRAM) for the SCWR will be identified and some preliminary analyses will be performed.

2. **Task 3.6.** On the basis of the results of the initial assessment, a safety concept will be developed. The aim is to develop a concept that will build on the strengths of the SCWR and effectively cope with any weakness that might be intrinsic with the concept. Since the SCWR will probably be deployed in the fourth decade of this century, if it is fully developed, a safety level at least comparable to the more advanced plant concepts (Westinghouse AP600/AP1000 and IRIS, GE ESBWR, Framatome-ANP SWR-1000) must be achieved.

   From a safety point of view the SCWR presents analogies both with the GE ESBWR (direct cycle system) with the Westinghouse AP600/AP1000 (dimensions of the pressure vessel) and with the IRIS reactor (compactness of the design compared to other plants). These three plant concepts will therefore be considered to develop a specific safety design for the SCWR.

3. **Task 3.5.** The SCWR adopts a direct cycle, but with a significant difference from the typical nuclear direct cycle in the fact that the system is once through. The current generation BWR direct cycle is based on a recirculation system: core flow is controlled with the flow control valves (FCVs) or with variable speed recirculation pumps, while feedwater control is based on a three-element control strategy. The ESBWR (which operates in natural circulation and does not employ recirculation pumps) apparently presents some more similarities with the SCWR, but it is still a recirculation system. A once through system such as the SCWR presents significant differences in operational behavior, that must be carefully assessed to develop an effective plant control system.

   While both PWRs and BWRs have some analogies in control strategy (both are based on a recirculation system, for the BWR the pressure vessel, for the PWR the steam generators), the SCWR will have some analogy with the IRIS reactor that Westinghouse is developing (and that adopts once-through steam generators). In defining the operation and control logic for the SCWR, useful insights will be extracted from the IRIS experience and the supercritical fossil fuel plants.

3.5.1. Reactor Pressure Vessel

The proposed vessel is very similar to a Westinghouse 3-Loop Plant. A conceptual layout is shown in Figure 36. The proposed vessel has an internal diameter of 4.41m and is 12.4 m tall. Data to perform an initial vessel nodalization using the RELAP code have been provided to INEEL. Some preliminary system data are summarized in Table 3.

Table 3 Main System Parameters for the SCWR

Core and Assembly Data	See Table 2
Thermal Power [MWt]	2700
Estimated Electric Power [MWe]	~1150
Vessel Dimensions	
Height [m]	12.4
ID/OD [m]	4.41 / 5.13
Barrel ID/OD [mm]	3.80 / 3.90
Thermal-Hydraulic Parameters	
Vessel Inlet Temperature [°C]	280
Vessel Outlet Temperature [°C]	450.3
Core Outlet Temperature [°C]	474
System Pressure [MPa]	25
Best Estimate Vessel Flow Rate [kg/s]	1567.87
Best Estimate Core Flow Rate [kg/s]	1473.8
Bypass Flow – Preliminary Estimates	
Head Cooling (%)	1
Core Bypass (%)	4
Outlet Nozzle Leakage (%)	1

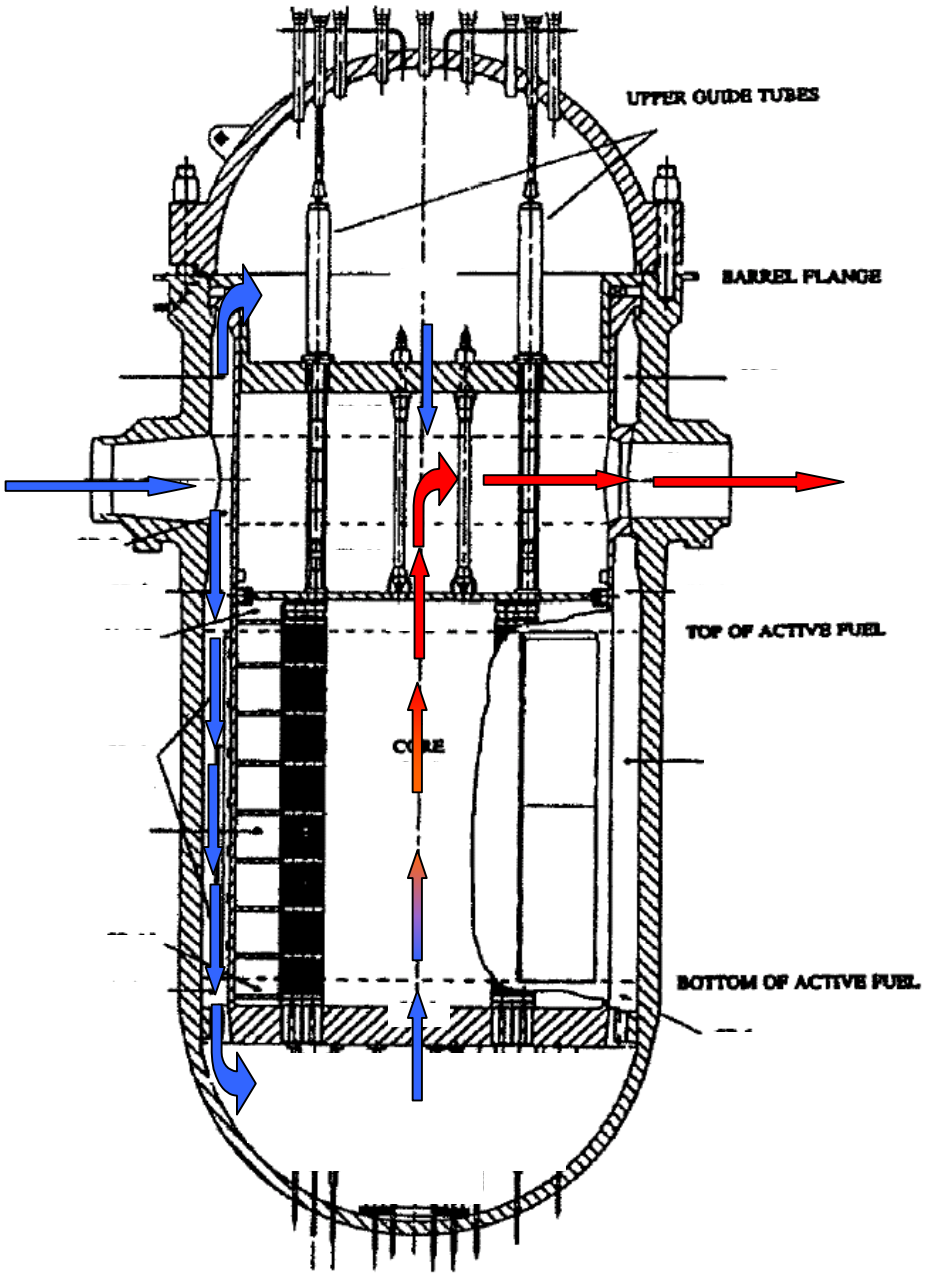

Figure 36. Reactor pressure vessel layout for the SCWR.

Feedwater is directed in the vessel through four inlet nozzles, to guarantee a uniform temperature and flow distribution in the vessel. Due to the low mass flow rates in the SCWR the feedwater nozzle and lines will be significantly smaller than in a PWRs vessel. The feedwater flow is then directed down the downcomer and then, through the lower plenum, into the core. In the core, the coolant is heated to high temperature, and then flows through the upper core plenum to the outlet nozzles. The upper head is maintained at cold conditions (feedwater temperature) by a small bypass through the upper downcomer from the feedwater flow. The flow path is very similar to a PWR. Compared to a direct cycle BWR, the

main difference (aside from the reduced dimensions) is the fact that the SCWR adopts a once-through system different from a BWR pressure vessel recirculation system.

The vessel is designed so to operate at feedwater temperature, except for the outlet nozzle that will operate at hot temperature. An internal review has been performed with vessel design experts to identify potential feasibility issues connected to the design of this pressure vessel and a program for addressing these issues have been developed. However, the scope of these activities would go beyond the purpose of this research, where the focus in on "feasibility issues": on the basis of the proposed program it is anticipated that problems related to the vessel design will not present insurmountable obstacles, and therefore the completion of this task has been postponed to a time when more advanced studies that go beyond a feasibility research will be considered.

Potential issues connected to the vessel design that were identified are briefly summarized in the following list:

1. The high temperature of the outlet nozzle will require the identification and eventual qualification of appropriate materials for nuclear applications.

2. The thermal gradient in the outlet nozzle region will have to be carefully considered: thermal gradients in PWRs vessel are typically negligible, but in the SCWR the difference in temperature between cold (feedwater) and hot (outlet nozzle conditions) coolant is more than 4 times that of a typical PWR (170°C versus ~40°C for a typical PWR). A finite element analysis of the nozzle (once an appropriate material for high temperature use is selected) would be required to properly assess this issue. The possibility of performing some investigation of this issue during the second year of the project is currently being discussed by INEEL and Westinghouse.

3. If the vessel design discussed above is not acceptable, different vessel design options could be considered, ranging from adopting a thermal sleeve (and maybe outside cooling) that maintains the outlet nozzles at colder conditions, to an exotic vessel design that features the "steam" pipe enclosed in the feedwater pipe so that the pressure boundary is maintained at cold temperature. For the thermal sleeve solution, the CANDU concepts for thermally isolating their pressure tubes from the SCW and cooling their pressure tubes on the outside would be a starting point. In the case of the double piping solution shown in the sketch of Figure 36, an appropriate plant design would be required to cope with a postulated concurrent failure of the double piping and its potential consequences. These solutions presents some feasibility issues of their own, but can be considered as interesting and innovative options in case the thermal stresses on the proposed reference solution are unacceptable.

4. Thermal transients on the pressure vessel might be significantly different from those of PWR (due to the adoption of a direct cycle) or BWR (due to the adoption of a once-through system). Since the design temperature is defined on the basis of the transient response of the system, it will be defined only following initial analyses on the SCWR.

5. The vessel is well within industry capabilities as far as dimensions and weight are concerned. The SCWR vessel weight will be comparable or lower than the weight of the advanced BWR plants (ESBWR, ABWR), the larger loop PWR plants (APWR) and integral reactor system plants (IRIS). The reactor pressure vessels for all of those plants are within current industry capabilities.

6. Other issues will eventually surface during the analyses phase (neutron fluence on the vessel, potential for rapid cooldown or heatup thermal transients) and will be addressed as they are identified.

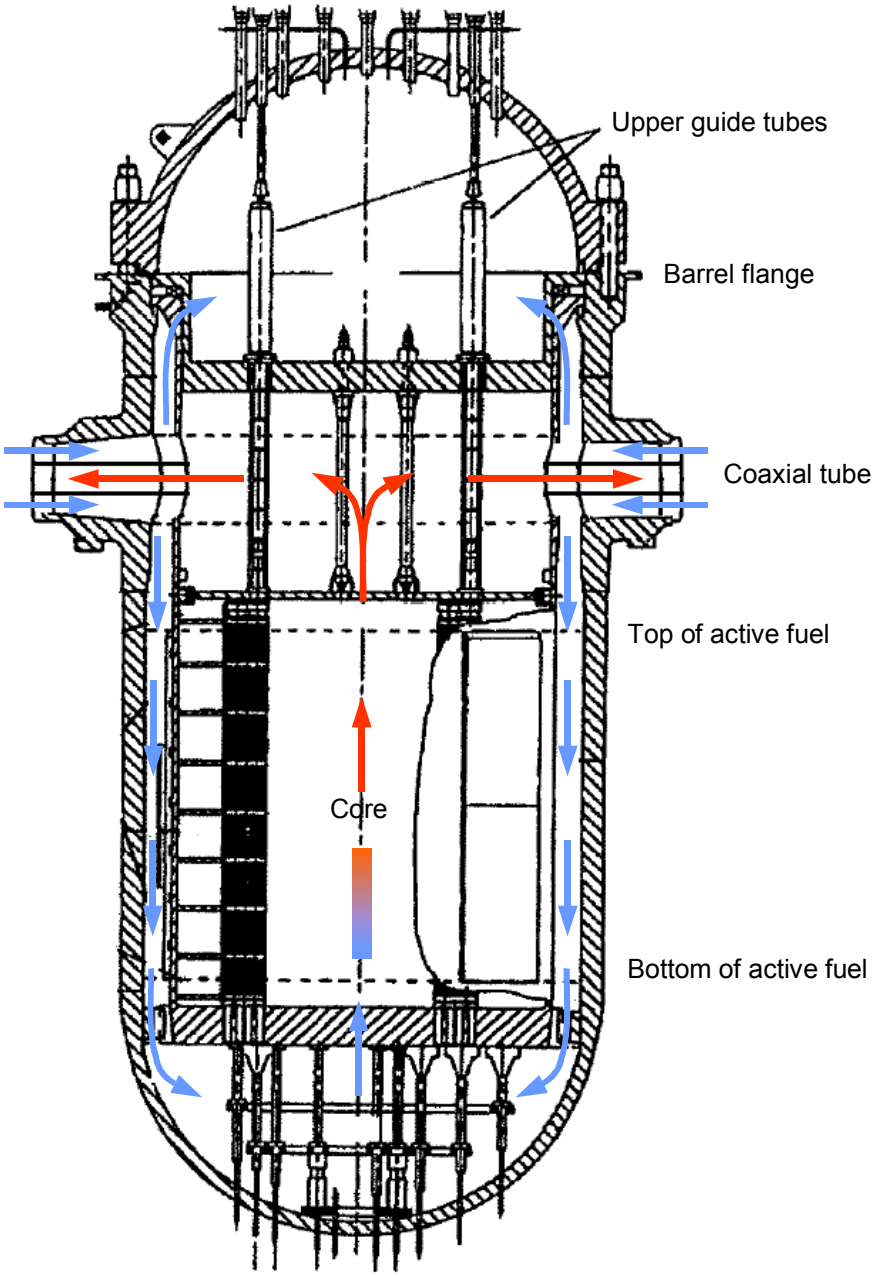

Figure 36. Double inlet-outlet piping SCWR pressure vessel layout.

References

- Berry, W. E., "The Corrosion Behavior of Fe-Cr-Ni Alloys in High Temperature Water" in NACE-4: High Temperature High Pressure Electrochemistry in Aqueous Solutions, D. de G. Jones, J.E. Slater and R.W. Staehle Eds., NACE, Houston TX (1973).
- Boukis, N., R. Landvatter, W. Habicht, G. Franz, "First Experimental SCWO Corrosion Results of Ni-Base Alloys Fabricated as Pressure Tubes and Exposed to Oxygen Containing Diluted Hydrochloric Acid at ≤ 450˚C, P=24 MPa", First Int. Workshop on Supercritical Water Oxidation, Jacksonville Florida, Feb 6-9 (1995).
- Boyd W. K., and H. A. Pray, "Corrosion of Stainless Steels in Supercritical Water", *Corrosion*, Vol. 13, p. 375 (1957).
- Cheng, X., T. Schulenberg, " Heat Transfer at Supercritical Pressures – Literature Review and Application to an HPLWR", FZKA-6609, Forschungszentrum Karlsruhe, 2001
- Duderstadt, J. J., and L. J. Hamilton, *Nuclear Reactor Analysis*, p.563, John Wiley & Sons, Inc., 1976.
- Hattori, T., and H. Anada, K. Abe and M. Harada: "Study of Fuel Cladding Materials for Supercritical Pressure Light Water Cooled Reactors", Proceedings of the 1st Int. Symp. on Supercritical Water-Cooled Reactors, Design and Technology (SCR-2000), Tokyo, Japan, Nov. 6-9 (2000).
- Heusner, G., et al., "A European Development Program for a High Performance Light Water Reactor (HPLWR)", Proc. of SCR-2000, Tokyo, Nov. 6-8, 2000
- Knief, R. A., *Nuclear Engineering*, pp.262-268, Hemisphere Publishing Corporation, 1992.
- MacDonald, P., J. Buongiorno, C.Davis, K. Weaver, R. Latanison, B. Mitton, G. Was, L. Oriani, M. Carelli, D. Paramonov, L. Conway, "Feasibility Study of Supercritical Light Water Cooled Reactors – Progress Report for Year 1- 1st Quarter", NERI 2001-001, INEEL/EXT-02-00107, September-December 2001
- MacDonald, P., J. Buongiorno, C.Davis, K. Weaver, R. Latanison, B. Mitton, G. Was, L. Oriani, M. Carelli, D. Paramonov, L. Conway, "Feasibility Study of Supercritical Light Water Cooled Reactors – Progress Report for Year 1- 2nd Quarter", NERI 2001-001, INEEL/EXT-02-00759, January-March 2002
- MacDonald, P., J. Buongiorno, C.Davis, K. Weaver, R. Latanison, B. Mitton, G. Was, L. Oriani, M. Carelli, D. Paramonov, L. Conway, "Feasibility Study of Supercritical Light Water Cooled Reactors – Progress Report for Year 1- 3rd Quarter", NERI 2001-001, INEEL/EXT-02-00925, April-June 2002
- Mitton, D. B., J. C. Orzalli and R. M. Latanision, *Corrosion in Supercritical Water Oxidation Systems,* 12th ICPWS, p. 638, Begell House, New York, NY (1995).
- Oka, Y., S Koshizuka, " Supercritical-Pressure, Once-through Cycle Light Water Cooled Reactor Concept", Journal of Nuclear Science and Technology, Vol. 38, No. 12, pp. 1081-1089, 2001
- Oka, Y., S Koshizuka, "Design Concept of Once-through Cycle Supercritical Pressure Light Water Cooled Reactor", Proc. of SCR-2000, Tokyo, Nov 6-8, 2000
- Spinks, N., et al., "Thermo-Economic Assessment of Advanced, High-Temperature CANDU Reactors", Proc. of 10th International Conference on Nuclear Engineering, ICONE10, Arlington, VA, April 14-18, 2002
- Stewart, C.W., et al., "VIPRE-01: A Thermal-Hydraulic Code for Reactor Cores," Volumes 1-4, Rev 3, NP-2511-CCM-A, August 1989.
- Tebbal, S., and R. D. Kane, "Materials Selection in Hydrothermal Oxidation Processes", *Corrosion 98*, Paper 413, NACE, Houston, TX (1998).

- Wozaldo, G. P., and W. L. Pearl, “General Corrosion of Stainless Steels and Nickel Base Alloys Exposed Isothermally in Superheated Steam”, *Corrosion,* Vol. 21, p. 355 (1965).

Project Schedule

Task	Activity	Description	Year 1	Year 2	Year 3
Task 1		Fuel-cycle Neutronic Analysis and Reactor Core Design (INEEL)			
	1.1	Reactivity Swing Analysis			
	1.2	Actinide Discharge and Isotopic Evaluation			
	1.3	Reactivity Coefficient Calculations			
	1.4	Peaking Factors and Reactor Control			
Task 2		Fuel Cladding and Structural Material Corrosion and Stress Corrosion Cracking Studies (University of Michigan, MIT)			
	2.1	Identification of Most Promising Materials (MIT)			
	2.2	Design and Construction of an Out-of-pile Supercritical Water Test Facility (U-Mich)			
	2.3	Corrosion and Stress Corrosion Cracking Behavior of Candidate Materials (U-Mich, MIT)			
	2.4	Radiation Stability of Candidate Alloys (U-Mich)			
	2.5	Modeling of Corrosion and stress Corrosion Cracking in Supercritical Water (U-Mich, MIT)			
Task 3		Plant Engineering and Reactor Safety Analysis (Westinghouse and INEEL)			
	3.1	Conceptual Design of the Reactor Coolant System (Westinghouse)			
	3.2	Definition of the Thermal/Mechanical Design Limits			
	3.3	Core Thermal-hydraulic Design (Westinghouse)			
	3.4	Evaluation of Coupled Thermal-hydraulic/Neutronic Oscillations (INEEL)			
	3.5	Plant Configuration and Operation (Westinghouse)			
	3.6	Establish the Conceptual Design of Required Safety Systems and Define their Performance Parameters (Westinghouse)			
	3.7	Analysis of Anticipated Transients and Potential Accidents (INEEL)			
	3.8	Conceptual Layout of Reactor Containment, Fuel Handling, and Auxiliary Buildings (Westinghouse)			
	3.9	Economic Analysis (Westinghouse)			

Budget and Actual Costs for Year 1

INEEL

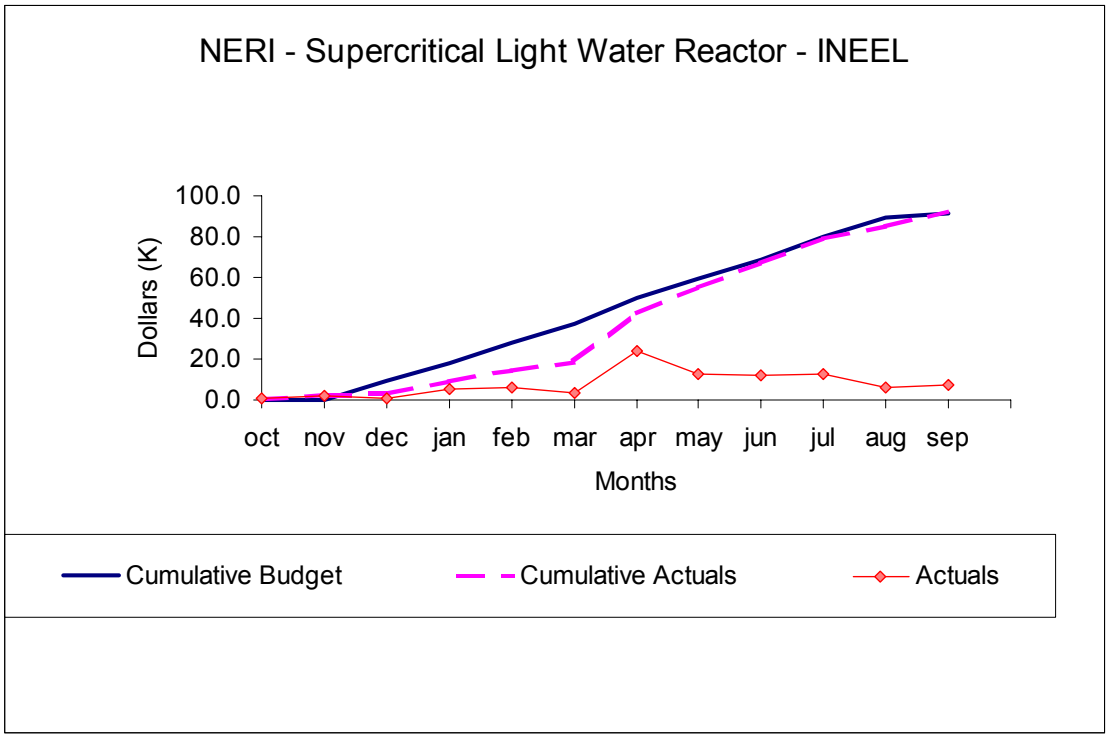

MIT

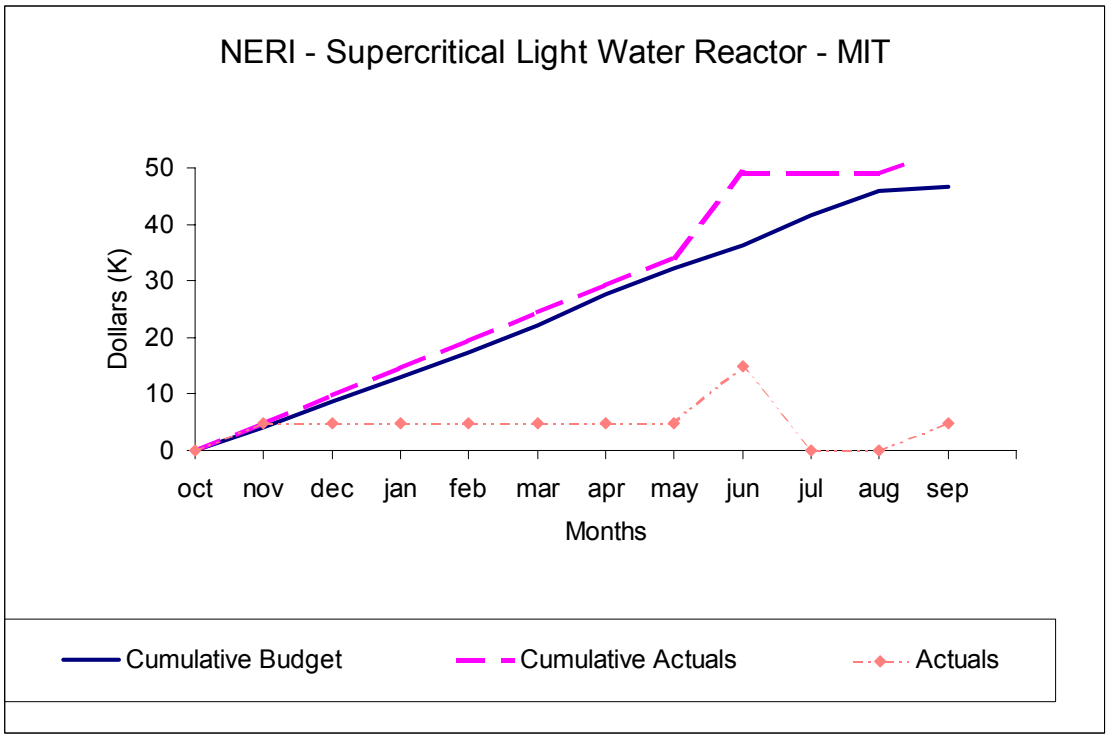

University of Michigan

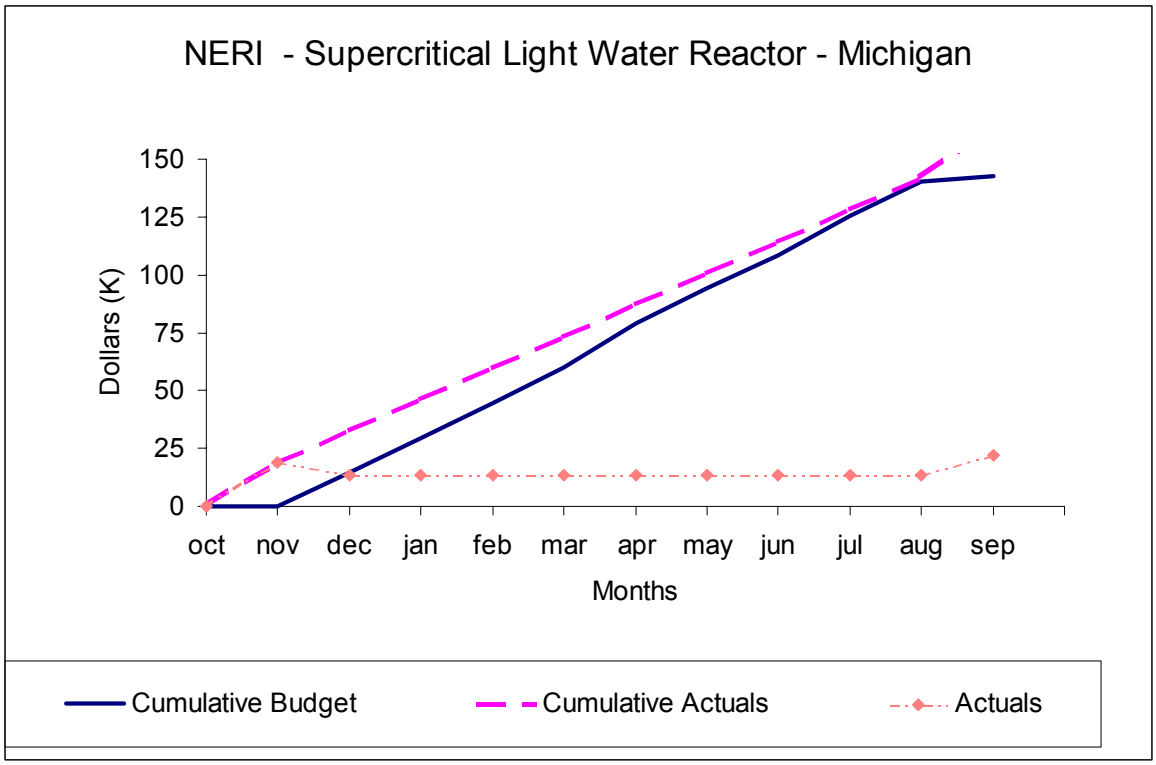

Westinghouse Electric Co.

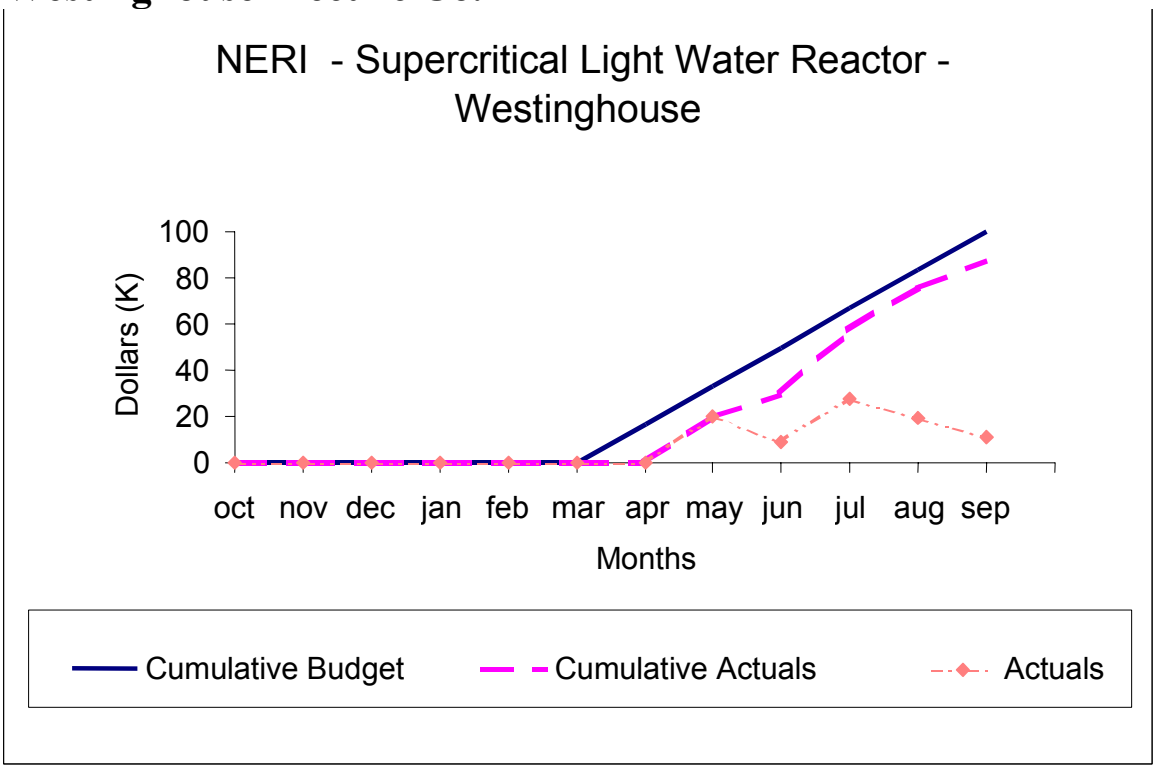

Appendix A. Nomenclature, Subscripts, and Acronyms for Section 3

Nomenclature

Cp	Heat Capacity [KJ/kg C]
Dh	Hydraulic Diameter [m]
G	Mass Velocity [kg/m^{2}s]
H	Specific Enthalpy [KJ/kg]
Ht	Heat Transfer coefficient [KW/m^2 C]
L	Channel Length
Nu	Nusselt Number
P	Pressure [MPa]
P/D	Pitch-over-Diameter Ratio
Pr	Prandtl Number
Q"	Heat Flux [W/m^2]
Re	Reynolds Number
T	Temperature [C]
μ	Viscosity [Pa-s]
ρ	Density [kg/m^3]
Δh	Enthalpy difference [KJ/kg]

Subscripts

b	Bulk temperature properties
w	Wall temperature properties
In	Core Inlet value
Out	Core Outlet value

Acronyms

ABWR	Advanced BWR
Bishop	Bishop correlation
BWR	Boiling Water Reactor
CHF	Critical Heat Flux
DHF	Deterioration Heat Flux
DNB	Departure from Nucleate Boiling
MAT-I	Maximum Allowable Cladding Temperature for ANSI Condition-I events
MAT-II	Maximum Allowable Cladding Temperature for ANSI Condition-II events
MNCTR	Minimum Nominal Cladding Temperature Ratio
MDNBR	Minimum DNB Ratio
MDHFR	Minimum DHF Ratio
NSSS	Nuclear Steam Supply System
OK	Oka-Koshizuka correlation
PWR	Pressurized Water Reactor
SCWR	SuperCritical Water Reactor
SRP	Standard Review Plan (NUREG-0800)

INEEL/EXT-02-01330

Feasibility Study of Supercritical Light Water Cooled Fast Reactors for Actinide Burning and Electric Power Production

Nuclear Energy Research Initiative Project 2001-001

Progress Report for Work Through September 2002

4th Quarterly Report

Principal Investigators:
Philip MacDonald, Dr. Jacopo Buongiorno, Cliff Davis, and Dr. Kevan Weaver
Telephone: 208-526-9634
Fax: 208-526-2930
Email: pem@inel.gov

Collaborating Organizations:
Massachusetts Institute of Technology
Principal Investigators: Professor Ron Latanision and Dr. Bryce Mitton

University of Michigan
Principal Investigator: Professor Gary Was

Westinghouse Electric Company
Principal Investigators: Drs. Luca Oriani, Mario Carelli, and Dmitry Paramonov, and Lawrence Conway